Robust Coordinated Hybrid Source Seeking with Obstacle Avoidance in Multi-Vehicle Autonomous Systems

Jorge I. Poveda, Mouhacine Benosman, Andrew R. Teel, Ricardo. G. Sanfelice

Abstract—In multi-vehicle autonomous systems that operate under unknown or adversarial environments, it is a challenging task to simultaneously achieve source seeking and obstacle avoidance. Indeed, even for single-vehicle systems, smooth time-invariant feedback controllers based on navigation or barrier functions have been shown to be highly susceptible to arbitrarily small jamming signals that can induce instability in the closed-loop system, or that are able to stabilize spurious equilibria in the operational space. When the location of the source is further unknown, adaptive smooth source seeking dynamics based on averaging theory may suffer from similar limitations. In this paper, we address this problem by introducing a class of novel distributed hybrid model-free controllers, that achieve robust source seeking and obstacle avoidance in multi-vehicle autonomous systems, with vehicles characterized by nonlinear continuous-time dynamics stabilizable by hybrid feedback. The hybrid source seeking law switches between a family of cooperative gradientfree controllers, derived from potential fields that satisfy mild invexity assumptions. The stability and robustness properties of the closed-loop system are analyzed using Lyapunov tools and singular perturbation theory for setvalued hybrid dynamical systems. The theoretical results are validated via numerical and experimental tests.

I. INTRODUCTION

N several applications, such as surveillance, target localization, or sensor deployment, it is of interest to have fully autonomous vehicles and mobile robots equipped with sensing and actuation capabilities, operating in hazardous environments that could be too dangerous for humans. Many of these navigation and exploration problems can be cast as source seeking problems [1]–[3], where the vehicles aim to

J. I. Poveda is with the Department of Electrical, Computer and Energy Engineering, University of Colorado, Boulder, CO. E-mail: jorge.poveda@colorado.edu. M. Benosman is with Mitsubishi Electric Research Laboratories, Cambridge, MA. E-mail: m.benosman@ieee.org. A. R. Teel is with the Department of Electrical and Computer Engineering, University of California, Santa Barbara, CA. E-mail:teel@ucsb.edu. R. G. Sanfelice is with the Department of Electrical and Computer Engunering, University of California, Santa Cruz, CA. E-mail: ricardo@ucsc.edu.

Earlier, partial results of this paper were partially presented at the American Control Conference, in Milwaukee, WI, USA, 2018.

J. I. Poveda has been partially supported by the NSF grant no. CNS-1947613 and by the ASIRT CU Boulder seed grant. M. Benosman has been solely funded by MERL. A . R. Teel has been partially supported by AFOSR grant no. FA9550-18-1-0246. R. G. Sanfelice has been partially supported by NSF grants no. ECS-1710621 and CNS-1544396, by AFOSR grants no. FA9550-16-1-0015, no. FA9550-19-1-0053, and no. FA9550-19-1-0169, and by CITRIS and the Banatao Institute at the University of California.

localize a point in the space where a particular measurable signal attains its maximum or minimum value. This signal may correspond to the chemical concentration of a hazardous substance, radiation coming from nuclear leaks, acoustic fields, etc. In all these scenarios, the precise mathematical model of the signal and/or its gradient is unknown, which precludes the implementation of standard gradient-based methods.

Several source seeking algorithms have been developed during the last 20 years. For example, in obstacle-free environments, source seeking controllers based on multi-function evaluations have been studied in [1], [4] and [3]. Continuous-time approaches based on extremum seeking dynamics [5] were pioneered in [6], and further studied in [7]–[10]. Hybrid controllers for obstacle-free source seeking problems in three-dimensional environments were studied in [11], and smooth source dynamics for unicycles were presented in [12]. Similarly, adaptive and cooperative navigation laws for *multivehicle systems* (MVS) operating in obstacle-free environments have also been considered in [3], [13]–[15] and [16].

The existing results in the literature have provided significant insight into the design of algorithms for source seeking and obstacle avoidance problems. However, in this setting, one of the main challenges is the design of feedback laws that are able to simultaneously achieve obstacle avoidance and global (or semi-global) stabilization of the source of the signal, under the presence of arbitrarily small, and therefore undetectable, additive adversarial jamming signals. As discussed in [17, Corollary 2.2], [18, Thm 6.5], and [19], this problem is not trivial mainly because of the topological obstructions induced by the obstacle, which preclude the global (or semi-global) robust stabilization of any given target point (e.g., the source) by using smooth feedback control laws, even if there is only one obstacle in the space. This impossibility result stems from the fact that the domain of attraction of an equilibrium point in asymptotically stable time-invariant vector fields must be diffeomorphic to the Euclidean space, see [19, pp. 558]. Naturally, in some cases this limitation extends to time-varying feedback controllers whose stability properties are completely inherited from a smooth time-invariant system, as it is the case in many approaches based on averaging theory [20]. To circumvent these limitations, most of the results in the literature have focused on achieving only local or almost global convergence results, where the set of initial conditions from which source seeking is not achieved corresponds to a set of measure zero; see [9], [21], [22]. However, as shown in [18, Thm 6.5] and [19], when the system is subject to

arbitrarily small additive adversarial disturbances, the set of initial conditions from which convergence is not achieved is not a set of measure zero anymore. Moreover, with the notable exception of [9], previous results in the literature of obstacle avoidance require direct access to the gradient (or a perturbed version of the gradient) of the potential field, and have considered simplified point-mass vehicle dynamics. Other model-based approaches have focused on achieving safe navigation, as opposed to source seeking, by using triangular partitions [23] and barrier functions for safety [24]. However, to the knowledge of the authors, how to design *model-free* feedback controllers that simultaneously achieve *robust* source seeking and obstacle avoidance in MVS with general nonlinear dynamics remains an open problem.

In this paper, we address this challenge by considering a novel class of model-free source seeking dynamics for obstacle avoidance based on *cooperative* synergistic Lyapunov functions and averaging theory for hybrid systems. In particular, the following are the main contributions of the paper:

- (a) We show in Proposition 1 and Example 1, that a common smooth and model-free averaging-based controller can fail to achieve obstacle avoidance and source seeking under a class of additive and arbitrarily small adversarial jamming signals able to stabilize spurious equilibria of the average dynamics. To address this issue, we develop a novel robust hybrid feedback navigation law that switches between a family of *model-free* controllers using a hysteresis rule, aiming to robustly steer a vehicle away from the obstacle and towards the source of the signal using only *measurements* of the intensity of the potential field. The convergence result is presented in Theorem 1. As opposed to stochastic approaches, such as those studied in [25] and [2], our setting is deterministic, which allows us to establish *sure* robust (as opposed to *almost sure*) source seeking and obstacle avoidance.
- (b) We show that the hybrid model-free controllers can be extended to MVS with a leader-follower structure, where only a subset of the vehicles is able to sense the intensity signal, and we provide sufficient conditions on the potential fields to guarantee obstacle avoidance and convergence to a particular pre-defined formation around the source. The result is presented in Theorem 2, and exploits a class of *cooperative* synergistic Lyapunov functions. Unlike the results presented in the conference paper [26], the results of this paper also guarantee global obstacle avoidance for the followers.
- (c) To extend the results of items (a) and (b) to vehicles with general nonlinear dynamics, we further study a novel multitime scale hybrid approach suitable for vehicles with dynamics satisfying a mild hybrid stabilizability assumption. To illustrate that non-holonomic vehicle systems satisfy this assumption, and inspired by the results of [27], we construct a hybrid feedback controller that achieves robust global stabilization of position and orientation in unicycles. By interconnecting this hybrid controller with the hybrid source seeking dynamics, we establish in Theorem 3 a convergence result for the closed-loop system using tools from singular perturbation theory for hybrid dynamical systems [28].
- (d) Finally, as a proof of concept, we validate in Section VII the practical feasibility of our theoretical results via numerical

and experimental tests in a TurtleBot platform.

To the best of our knowledge, the results of this paper correspond to the first adaptive averaging-based hybrid controllers able to achieve robust model-free (semi) global practical source seeking and obstacle avoidance in MVS having general nonlinear dynamics that are stabilizable by using hybrid feedback. Earlier, partial results were presented in the conference paper [26], which studied a hybrid source seeking controller designed for a single-vehicle velocity-actuated system.

II. NOTATION AND PRELIMINARIES

Given a compact set $\mathcal{A} \subset \mathbb{R}^n$ and a vector $z \in \mathbb{R}^n$, we use $|z|_{\mathcal{A}} := \min_{s \in \mathcal{A}} ||z - s||_2$ to denote the minimum distance of z to \mathcal{A} . A set-valued mapping $M:\mathbb{R}^p \rightrightarrows \mathbb{R}^n$ is said to be outer semicontinuous (OSC) at z if for each sequence $\{z_i, s_i\} \to (z, s) \in \mathbb{R}^p \times \mathbb{R}^n$ satisfying $s_i \in M(z_i)$ for all $i \in \mathbb{Z}_{\geq 0}$, we have $s \in M(z)$. A mapping M is locally bounded (LB) at z if there exists an open neighborhood $N_z \subset \mathbb{R}^p$ of z such that $M(N_z)$ is bounded. The mapping M is OSC and LB relative to a set $K \subset \mathbb{R}^p$ if M is OSC for all $z \in K$ and $M(K) := \bigcup_{z \in K} M(x)$ is bounded. A function $f : \mathbb{R}^p \to \mathbb{R}$ is said to be radially unbounded if $f(z) \to \infty$ as $|z| \to \infty$. Given a set $K \subset \mathbb{R}^p$, we use \overline{K} to denote its closure, $\mathbb{R}^n \backslash K$ to denote its complement, $\overline{\operatorname{co}}K$ to denote its closed convex hull, and $K^N := K \times ... \times K$ to denote its N-cartesian product. We use $\mathbb{S}^1 := \{z \in \mathbb{R}^2 : z_1^2 + z_2^2 = 1\}$ to denote the unit circle in \mathbb{R}^2 , and $r\mathbb{B}$ to denote a closed ball in the Euclidean space, of radius r > 0, and centered at the origin. We use I_n to denote the identity matrix of dimension $n \times n$, e_i to denote the unitary vector with i^{th} entry equal to 1, and $\mathbf{c}_N \in \mathbb{R}^N$ to denote the vector with all entries equal to $c \in \mathbb{R}$. Also, for each vector $\alpha \in \mathbb{R}^N$ we use $I(\alpha)$ to denote the diagonal matrix whose diagonal elements correspond to the entries of α . For any pair of vectors $x = [x_1, x_2]^{\top}$ and $y = [y_1, y_2]^{\top}$, we define $x^c :=$ $[x_1, -x_2]^{\top}$ and the operation $x \ominus y := [x_1y_1 - x_2y_2, x_2y_1 +$ x_1y_2 ^{\top}. An undirected unweighted graph is represented by $\mathcal{G} = \{\mathcal{V}, \mathcal{E}\}\$, where $\mathcal{V} \subset \{1, 2, \dots, N\}$ is the set of nodes, and $\mathcal{E} \subset \mathcal{V} \times \mathcal{V}$ is the set of edges. A function $\alpha : \mathbb{R}_{\geq 0} \to \mathbb{R}_{\geq 0}$ is of class \mathcal{K}_{∞} if it is zero at zero, continuous, strictly increasing, and unbounded. A function $\beta: \mathbb{R}_{>0} \times \mathbb{R}_{>0} \to \mathbb{R}_{>0}$ is of class \mathcal{KL} if it is nondecreasing in its first argument, nonincreasing in its second argument, $\lim_{r\to 0^+} \beta(r,s) = 0$ for each $s \in \mathbb{R}_{\geq 0}$, and $\lim_{s\to\infty}\beta(r,s)=0$ for each $r\in\mathbb{R}_{>0}$. For a compact set \mathcal{A} contained in an open set \mathcal{U} , a continuous function $\tilde{\omega}:\mathcal{U}\to$ $\mathbb{R}_{>0}$ is a proper indicator of \mathcal{A} on \mathcal{U} if $\tilde{\omega}(z)=0$ if and only if $z \in \mathcal{A}$, and $\tilde{\omega}(z_i) \to \infty$ when $i \to \infty$ if either $|z_i| \to \infty$, or the sequence $\{z_i\}_{i=1}^{\infty}$ approaches the boundary of \mathcal{U} .

In this paper, we will consider dynamical systems with continuous-time and discrete-time dynamics, called *hybrid dynamical systems* (HDS) [29]. A HDS with state $z \in \mathbb{R}^n$ is characterized by its data $\mathcal{H} := (C, F, D, G)$, and the dynamics

$$z \in C, \qquad \dot{z} = F(z),$$
 (1a)

$$z \in D, \qquad z^+ \in G(z),$$
 (1b)

where the mappings $F: \mathbb{R}^n \to \mathbb{R}^n$ and $G: \mathbb{R}^n \rightrightarrows \mathbb{R}^n$, called the flow map and the jump map, respectively, describe the

evolution of the state z when it belongs to the flow set C, and the jump set D, respectively. We will always consider HDS that satisfy the following Hybrid Basic Conditions:

- (C1) The sets C and D are closed.
- (C2) F is continuous on C.
- (C3) G is OSC and LB relative to D, and for every $z \in D$ the set G(z) is nonempty.

Solutions to system (1) are parametrized by a continuoustime index $t \in \mathbb{R}_{\geq 0}$ that increases continuously whenever the system flows according to (1a), and a discrete-time index $j \in \mathbb{Z}_{\geq 0}$ that increases by one whenever the system jumps according (1b). Thus, solutions to (1) are defined on *hybrid* time domains. Solutions with an unbounded time domain are said to be complete. Further details on hybrid time domains and solutions to HDS can be found in [29, Ch. 2].

The following two stability definitions, which also apply to continuous-time systems (i.e., $D = \emptyset$), discrete-time systems (i.e., $C = \emptyset$), and HDS will be used throughout this paper.

Definition 1: A compact set $A \subset \mathbb{R}^n$ is said to be uniformly globally asymptotically stable (UGAS) for the HDS \mathcal{H} if there exists a $\beta \in \mathcal{KL}$ such that all solutions z to \mathcal{H} satisfy the bound $|z(t,j)|_A \leq \beta(|z(0,0)|_A,t+j)$, for all $(t,j) \in \text{dom}(z)$. \square

Definition 2: For a HDS parametrized by a constant $\varepsilon \in \mathbb{R}_{>0}$, and denoted as $\mathcal{H}_{\varepsilon} := \{C_{\varepsilon}, F_{\varepsilon}, D_{\varepsilon}, G_{\varepsilon}\}$, a compact set $\mathcal{A} \subset \mathbb{R}^n$ is said to be semi-globally practically asymptotically stable (SGPAS) as $\varepsilon \to 0^+$ if there exists a function $\beta \in \mathcal{KL}$ such that the following holds: for each $\Delta > 0$ and $\nu > 0$ there exists $\varepsilon^* > 0$ such that for each $\varepsilon \in (0, \varepsilon^*)$ every solution z of $\mathcal{H}_{\varepsilon}$ with $|z(0,0)|_{\mathcal{A}} \leq \Delta$ also satisfies the bound $|z(t,j)|_{\mathcal{A}} \leq \beta(|z(0,0)|_{\mathcal{A}}, t+j) + \nu$, for all $(t,j) \in \text{dom}(z)$.

When the sets C_{ε} and D_{ε} are compact, SGPAS is equivalent to global practical asymptotic stability (GPAS). The following lemma corresponds to [29, Thm. 7.21].

Lemma 1: Let \mathcal{H} be a HDS of the form (1) satisfying the Basic Conditions, and rendering a nonempty compact set $\mathcal{A} \subset \mathbb{R}^n$ UGAS. Then, for the inflated HDS $\mathcal{H}_{\varepsilon}$ with data given by

$$F_{\varepsilon}(x) := \overline{\operatorname{co}} \ F((x + \varepsilon \mathbb{B}) \cap C) + \varepsilon \mathbb{B}$$

$$G_{\varepsilon}(x) := \{ v \in \mathbb{R}^{n} : v \in g + \varepsilon \mathbb{B}, g \in G((x + \varepsilon \mathbb{B}) \cap D) \}$$

$$C_{\varepsilon} := \{ x \in \mathbb{R}^{n} : (x + \varepsilon \mathbb{B}) \cap C \neq \emptyset \}$$

$$D_{\varepsilon} := \{ x \in \mathbb{R}^{n} : (x + \varepsilon \mathbb{B}) \cap D \neq \emptyset \},$$

the set \mathcal{A} is SGPAS as $\varepsilon \mapsto 0^+$.

III. PROBLEM STATEMENT AND MOTIVATIONAL EXAMPLE

Consider a group of N vehicles in \mathbb{R}^2 , each vehicle modeled by the dynamics

$$\dot{p}_i = u_i, \qquad \forall \ i \in \ \mathcal{V} := \{1, \dots, N\},\tag{2}$$

where $p_i \in \mathbb{R}^2$ represents the position, and $u_i \in \mathbb{R}^2$ represents the velocity input. Point mass models of the form (2) have been extensively studied in the literature of source seeking; see [6], [10]. We are interested in designing a *robust* and *model-free* feedback law u_i that steers the vehicles, in a coordinated way, towards a neighborhood of the maximizer of an unknown but measurable potential field J, generating vehicle trajectories that simultaneously avoid a given obstacle \mathcal{N} . For the purpose

of analysis, we consider potential functions that satisfy the following assumption.

Assumption 1: The potential function $J: \mathbb{R}^2 \to \mathbb{R}$ is continuously differentiable, -J is radially unbounded, and the set of global maximizers of J, given by

$$\mathcal{A}_J := \{ p^* \in \mathbb{R}^2 : J(p^*) \ge J(p), \ \forall \ p \in \mathbb{R}^2 \},$$
 (3)

is not empty, and also coincides with the set of critical points $\mathcal{Z}_{\nabla J}:=\{p^*\in\mathbb{R}^2:\nabla J(p^*)=0\}$, i.e., -J is an invex function [30].

Assumption 1 is weaker than previous assumptions in the literature of source seeking that considered quadratic functions [6], [8]–[10], [31] or strongly concave potential fields [4]. In particular, convexity of -J is not assumed. Similar potential fields have been studied in [11].

To motivate our results, we first study a common smooth averaging-based navigation law for the case when there is only one vehicle, i.e., $\mathcal{V} := \{1\}$, and we drop the subindex i in (2).

A. Smooth Source Seeking Dynamics: The Obstacle-Free Case

In an obstacle-free space, we can consider the following model-free source seeking control law:

$$u := a\omega R\mu + k\xi, \qquad R := \begin{bmatrix} 0 & 1 \\ -1 & 0 \end{bmatrix}, \tag{4}$$

where $k:=\sigma\bar{\omega}$, and $[\sigma,\bar{\omega},a,\omega]^{\top}\in\mathbb{R}^4_{>0}$ is a vector of tunable parameters. The auxiliary states $\xi\in\mathbb{R}^2$ and $\mu\in\mathbb{R}^2$ are generated by the dynamics

$$\begin{bmatrix} \dot{\xi} \\ \dot{\mu} \end{bmatrix} = \begin{bmatrix} -\bar{\omega} \left(\xi - \frac{2}{a} J(p) \mu \right) \\ \omega R \mu \end{bmatrix}, \quad (\xi, \mu) \in \mathbb{R}^2 \times \mathbb{S}^1. \quad (5)$$

This feedback law is similar to those considered in [10] and [6, Ch. 2], with the subtle difference that we generate the excitation signal μ using a time-invariant oscillator, whose solutions can be explicitly computed as

$$\mu(t) = \exp(\omega R t) \mu(0) = \begin{bmatrix} \cos(\omega t) & \sin(\omega t) \\ -\sin(\omega t) & \cos(\omega t) \end{bmatrix} \begin{bmatrix} \mu_1(0) \\ \mu_2(0) \\ 0 \end{bmatrix}.$$

Since $\frac{d(\mu^{\top}\mu)}{dt}=0$, it follows that \mathbb{S}^1 is forward invariant for any $\omega>0$. The low-pass filter of (5) is solely used to improve the transient performance of the algorithm, and it can be safely removed without altering the stability properties of the controller. However, we retain the filter in this section to show that, in general, it does not improve the robustness properties of the controller under a class of arbitrarily small jamming signals.

The control law (4) can be analyzed following the ideas of [6, Ch. 2]. In particular, consider the change of variables $\tilde{p}:=p-a\mu$, and the new time scale $\tilde{\rho}=\bar{\omega}t$. With these new variables, the closed-loop system in the $\tilde{\rho}$ -time scale has the form

$$\dot{\tilde{p}} = \sigma \xi, \quad \dot{\xi} = -\xi + \frac{2}{a} J(\tilde{p} + a\mu)\mu, \quad \nu \dot{\mu} = R\mu, \tag{7}$$

where $\nu := \frac{\bar{\omega}}{\omega}$. When ν is sufficiently small, system (7) can be analyzed using averaging theory [20]. The average system is obtained by averaging the ξ -dynamics along the

$$J(\tilde{p} + a\mu) = J(\tilde{p}) + a \ \mu^{\top} \nabla J(\tilde{p}) + e_J, \tag{8}$$

where the term e_J is of order $O(a^2)$. The following lemma is instrumental to find the average dynamics of system (7). The proof follows directly by integration and application of trigonometric identities.

Lemma 2: Every solution of
$$\dot{\mu} = R\mu$$
 satisfies $\int_0^{2\pi} \mu(t) dt = \mathbf{0}_2$ and $\frac{1}{2\pi} \int_0^{2\pi} \mu(t) \mu(t)^{\top} dt = \frac{1}{2} I_2$.

Substituting (8) in (7), and taking the average of the ξ -dynamics over one period of μ , we obtain the average system in the $\tilde{\rho}$ -time scale with states $\xi^A \in \mathbb{R}^2$ and $\tilde{p}^A \in \mathbb{R}^2$:

$$\dot{\tilde{p}}^A = \sigma \xi^A, \quad \dot{\xi}^A = -\xi^A + \nabla J(\tilde{p}^A) + \tilde{e}_J, \tag{9}$$

where \tilde{e}_J is a term of order O(a). By further introducing a new time scale $\alpha:=\sigma\tilde{\rho}$, system (9) is in singular perturbation form (see [20]) whenever $\sigma>0$ is sufficiently small. The "boundary layer" dynamics are obtained by setting $\sigma=0$ in (9). With \tilde{p}^A constant, the equilibrium point $\xi^{A*}=\nabla J(\tilde{p}^A)+\tilde{e}_J$ is exponentially stable for the ξ^A -dynamics. The "reduced dynamics" are obtained after substituting ξ^A by its steady-state value ξ^{A*} in the \tilde{p} -dynamics, leading to

$$\dot{\tilde{z}} = \nabla J(\tilde{z}) + \tilde{e}_z, \tag{10}$$

where the new variable $\tilde{z} \in \mathbb{R}^2$ corresponds to the position of the vehicle, and \tilde{e}_z is of order $\mathcal{O}(a)$. This computation reveals that, under an appropriate tuning of the constants (σ, ν, a) , the feedback law (4) applied to the vehicle (2) approximates, on average and in the slowest time scale, a gradient flow with respect to the potential field J. For the average system (10) the following lemma can be readily established.

Lemma 3: Suppose that J satisfies Assumption 1. Then, if $\tilde{e}_z = 0$, system (10) renders the set \mathcal{A}_J UGAS. If \tilde{e}_z is of order $\mathcal{O}(a)$, system (10) renders the set \mathcal{A}_J SGPAS as $a \to 0^+$. \diamondsuit

Proof: Let $J^*:=J(\mathcal{A}_J)$. If $\tilde{e}_z=0$, UGAS follows by considering the Lyapunov function $V(\tilde{z})=-(J(\tilde{z})-J^*)$, which is radially unbounded and positive definite with respect to \mathcal{A}_J , and satisfies $\dot{V}=-|\nabla J(\tilde{z})|^2<0$ for all $\tilde{z}\notin\mathcal{A}_J$. If \tilde{e}_z is of order $\mathcal{O}(a)$, SGPAS follows by Lemma 1 and the observation that solutions of (10) on compact sets and for a>0 sufficiently small are also solutions of the differential inclusion $\dot{\tilde{z}}\in\overline{\text{co}}\ \nabla J(\tilde{z}+\varepsilon\mathbb{B})+\varepsilon\mathbb{B}$, with $\varepsilon>0$.

Once a UGAS or SGPAS property has been established for the slow average system (10), standard results for averaging and singular perturbation theory (e.g., [20, Thm. 1] or [32, Thm. 1]) can be invoked to establish SGPAS for the original model-free source seeking dynamics (7). Since the closed-loop system is modeled by a time-invariant continuous vector field, for each suitable tuning of the control parameters the existence of robustness margins with respect to small bounded additive disturbances on the states and dynamics can be readily established via Lemma 1.

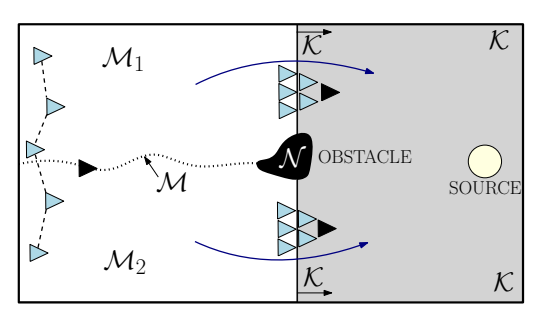


Fig. 1: A group of vehicles seeking the source of a signal, under the presence of the obstacle \mathcal{N} . For a smooth control law, the set \mathcal{M} represents the points where small perturbations can prevent the agents from converging to the source.

B. Smooth Source Seeking Under Obstacles and Small Adversarial Signals: An Impossibility Result

Whereas the feedback law (4) successfully solves the nominal source seeking problem when there are no obstacles in the space, the same algorithm can generate closed-loop systems with zero margins of robustness with respect to arbitrarily small jamming signals designed to stabilize spurious equilibria of the average dynamics (10). To illustrate this idea, consider Figure 1, where $\mathcal{N} \subset \mathbb{R}^2$ represents the obstacle, and the green triangles represent follower agents tracking the position of the leader, represented by a black triangle and the state $\tilde{z} \in \mathbb{R}^2$. Suppose that a feedback controller has been designed to globally steer the leader towards the source. Without loss of generality, the closed-loop dynamics can be written as

$$\dot{\tilde{z}} = f(\tilde{z}), \quad \tilde{z} \in \mathbb{R}^2 \backslash \mathcal{N}, \quad \tilde{z}(0) = \tilde{z}_0,$$
 (11)

where the function f is assumed to be locally bounded (possibly discontinuous), and where the existence of at least one complete (Carathéodory) solution [33, pp. 4] for all $\tilde{z}(0) \in \mathbb{R}^2 \backslash \mathcal{N}$ is assumed. Note that, since there is an obstacle in the space, there must exist a set $\mathcal{M} \subset \mathbb{R}^2$ such that, for initial conditions on each side of \mathcal{M} , i.e., in \mathcal{M}_1 or \mathcal{M}_2 (see Figure 1), the trajectories of the vehicle approach the set \mathcal{K} either from above the obstacle or from below it. For the obstacle avoidance problem this behavior is captured by the following assumption.

Assumption 2: There exists T > 0 such that for each $\rho > 0$ and each $\tilde{z}_0 \in \mathcal{M}$, where $\mathcal{M} := \overline{\mathcal{M}_1} \cap \overline{\mathcal{M}_2}$, there exist points $\tilde{z}_1(0), \tilde{z}_2(0) \in \{\tilde{z}_0\} + \rho \mathbb{B}$, for which there exist solutions \tilde{z}_1 and \tilde{z}_2 of (11), respectively, satisfying $\tilde{z}_1(t) \in \mathcal{M}_1 \backslash \mathcal{M}$ and $\tilde{z}_2(t) \in \mathcal{M}_2 \backslash \mathcal{M}$ for all $t \in [0, T]$.

A consequence of the behavior described by Assumption 2 is the existence of *arbitrarily small* adversarial jamming signals e that can force the solutions of the perturbed system

$$\dot{\tilde{z}} = f(\tilde{z} + e(t)), \quad \tilde{z}(0) = \tilde{z}_0 + e(0) \in \mathbb{R}^2 \backslash \mathcal{N}, \quad (12)$$

to remain in a neighborhood of the set \mathcal{M} . This can be established by the following proposition, which follows as a special case of [18, Thm. 6.5].

Proposition 1: Suppose that Assumption 2 holds. Then for each $\varepsilon, \rho', \rho'' > 0$, and every $\tilde{z}_0 \in \mathcal{M} + \varepsilon \mathbb{B}$ such that $\tilde{z}_0 + \rho' \mathbb{B} \subset \mathbb{R}^2 \backslash \mathcal{N}$ and $\tilde{z}_0 + \rho'' \mathbb{B} \subset (\mathcal{M}_1 \cup \mathcal{M}_2)$ there exist a piecewise

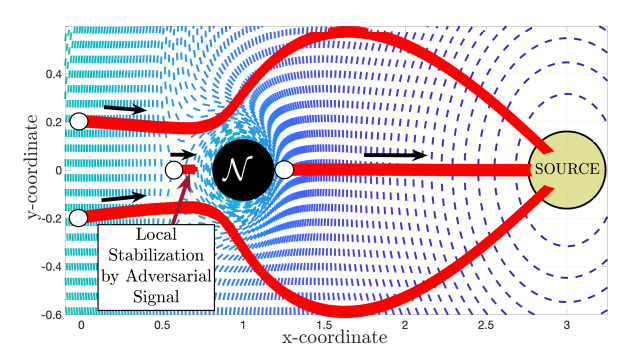


Fig. 2: Four trajectories of the dynamics (4) under the adversarial jamming signal e(t) of Example 1. The parameters of the simulation are selected as $\omega = 150$, $\bar{\omega} = 0.01$, $k = 1 \times 10^{-3}$, a = 0.01, $\rho = 0.035$, $\mu(0) = [1,0]^{\top}$, $\varepsilon = 1 \times 10^{-2}$.

constant function $e: \text{dom}(e) \to \varepsilon \mathbb{B}$ and a (Carathéodory) solution $\tilde{z}: \text{dom}(\tilde{z}) \to \mathbb{R}^2 \backslash \mathcal{N}$ to (12) such that

$$\tilde{z}(t) \in (\mathcal{M} + \varepsilon \mathbb{B}) \cap (\mathcal{M}_1 \cup \mathcal{M}_2) \cap (\tilde{z}_0 + \rho' \mathbb{B}),$$

for all $t \in [0, T')$ for some $T' \in (T^*, \infty]$, where dom $\tilde{z} = \text{dom } \tilde{e}$, $T^* = \min\{\rho', \rho''\}m^{-1}$, and $m = \sup\{1 + |f(\eta)| : \eta \in z_0 + \max\{\rho', \rho''\}\mathbb{B}\}$. If T' is finite, then $\lim_{t \to T'} \tilde{z}(t) \notin (\mathcal{M}_1 \cup \mathcal{M}_2) \cup (\tilde{z}(0) + \rho'\mathbb{B})$.

Given that the reduced average system (10) is of the form (11), a consequence of Proposition 1 is that the existence of obstacles in the operational space of the vehicle implies the existence of arbitrarily small (and therefore undetectable in practice) adversarial jamming signals e that could significantly deteriorate the stability properties of the system. In fact, the adversarial signal e can be designed to locally stabilize spurious equilibria that may emerge in gradient flows due to the combination of attractive fields and repulsive fields. This observation suggests that the signal e could also be designed to disrupt the stability properties of the model-free dynamics e (4) by (locally) stabilizing spurious equilibria of e (10). This is illustrated by the following example.

Example 1: Consider the dynamics (4), a potential field $J(x) = -(x-3)^2 - y^2$, and an obstacle located at the point (1,0). To "push" the vehicle away from the obstacle, we design an artificial "repulsive" function B(d(p)) as in [34], defined as $B(z):=(z-1)^2\log\left(\frac{1}{z}\right)$ if $z\in[0,1]$, and B(z):=0 if z>1, where $d:\mathbb{R}^2\to\mathbb{R}_{\geq0}$ is the distance function given by $d(p) = ((x_1 - 1)^2 + y^{\overline{2}})^{0.5} - \rho$ if $(x_1-1)^2+y^2>\rho^2$, and d(p)=0 otherwise. This construction generates a continuously differentiable potential field J(p) = J(p) - B(d(p)), which serves as input to the dynamics (5). Now, consider the uniformly bounded small adversarial jamming signal $e(t) := [-\varepsilon \delta_1(x(t) - 0.6), -\varepsilon \delta_2(y(t))]^{\top},$ where $\varepsilon > 0$, $\delta_i(z) := z$ if $|z| \le \overline{\delta}_i$, and $\delta_i(z) := 0$ otherwise, with $\bar{\delta}_1 = 0.15$ and $\bar{\delta}_2 = 0.05$. When this signal is added to the right hand side of (4), solutions starting sufficiently close to the point (0.6,0) are not able to reach the source. In fact, the adversarial signal e keeps the trajectory of the vehicle in a neighborhood of (0.6,0), which is a saddle point of J(p)and therefore a critical point of $\nabla \tilde{J}(p)$ (c.f. equation (10)). On the other hand, perturbed solutions starting sufficiently far

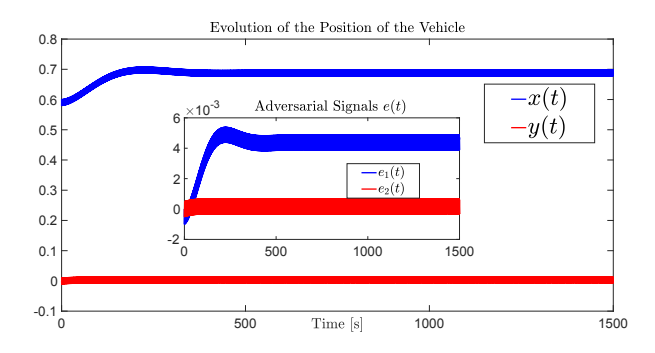


Fig. 3: Trajectories generated by (4) under the adversarial signal e(t), and initial condition close to (0.6, 0). The inset shows the evolution in time of the adversarial signals.

away from the saddle point achieve obstacle avoidance. This behavior is illustrated in Figure 2. The evolution in time of the adversarial signals and the position of the vehicle are shown in Figure 3.

Example 1 aims to illustrate a vulnerability that emerges in any smooth averaging-based source seeking algorithm that completely inherits its stability and convergence properties from standard gradient flows operating under obstacles in the space, and subject to adversarial environments. Indeed, it is well-known that similar vulnerabilities emerge in other stabilization problems under topological obstructions; see for instance [19], and [35]. Nevertheless, this limitation can be overcome if the smooth adaptive source seeking controller is substituted by a robust adaptive *hybrid* controller.

IV. ROBUST HYBRID SOURCE SEEKING WITH OBSTACLE AVOIDANCE FOR A SINGLE-VEHICLE SYSTEM

In this section, we present a model-free hybrid feedback law designed to achieve (semi) global (practical) source seeking and robust obstacle avoidance in vehicle systems with dynamics of the form (2). To simplify our presentation, we consider single-vehicle systems, and we defer to the next section the analysis of MVS.

A. Geometric Covering of the State Space

The main idea behind the hybrid source seeking algorithm is to cover the operational space of the vehicle by using multiple virtual sets, and to implement a different smooth model-free robust source seeking controller in each set, using an appropriate switching law. To do this, we first characterize the class of admissible obstacles $\mathcal N$ that we consider in this paper, which are those that can be contained in spheres and are located "sufficiently" away from the set $\mathcal A_J$ defined in Assumption 1.

Assumption 3: There exists $\rho \in \mathbb{R}_{>0}$ and $\varepsilon \in \mathbb{R}_{>0}$ such that the obstacle $\mathcal{N} \subset \mathbb{R}^2$ satisfies $\mathcal{N} \subset p_0 + \rho \mathbb{B}$ and $(p_0 + 2\rho\sqrt{2}\mathbb{B}) \cap (\mathcal{A}_J + \varepsilon \mathbb{B}) = \emptyset$, where $p_0 = [x_0, y_0]^\top \in \mathbb{R}^2$.

To achieve global obstacle avoidance, a covering of the operational space can be constructed as follows: For each $p_0 \in \mathbb{R}^2$ and $\rho > 0$, define the set

$$\mathcal{B}_{p_0,\rho} := \left\{ p \in \mathbb{R}^2 : \|p - p_0\|_1 \le 2\rho\sqrt{2} \right\},$$
 (13)

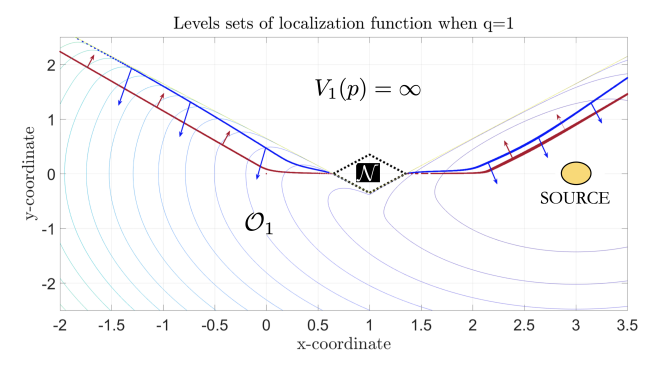


Fig. 4: Space \mathcal{O}_q with q=1. The blue arrows indicate the flow set (18a), and the red arrows indicate the jump set (18b). The box contains $\mathcal{B}_{p_0,\rho}$.

and note that $\{p_0\} + \rho \mathbb{B} \subset \mathcal{B}_{p_0,\rho} \subset \{p_0\} + 2\rho\sqrt{2}\mathbb{B}$. Consider the sets

$$L_{1a} := \left\{ [x, y]^{\top} \in \mathbb{R}^2 : \ y < -x + y_0 + x_0 - 2\rho\sqrt{2} \right\},$$

$$L_{1b} := \left\{ [x, y]^{\top} \in \mathbb{R}^2 : \ y < x + y_0 + x_0 + 2\rho\sqrt{2} \right\},$$

$$L_{2a} := \left\{ [x, y]^{\top} \in \mathbb{R}^2 : \ y > x + y_0 + x_0 - 2\rho\sqrt{2} \right\},$$

$$L_{2b} := \left\{ [x, y]^{\top} \in \mathbb{R}^2 : \ y > -x + y_0 + x_0 + 2\rho\sqrt{2} \right\},$$

and define the virtual sets

$$\mathcal{O}_1 := L_{1a} \cup L_{1b}, \quad \mathcal{O}_2 := L_{2a} \cup L_{2b}, \quad \mathcal{O} := \mathcal{O}_1 \cup \mathcal{O}_2.$$
 (14)

Note that $\mathcal{O} = \mathbb{R}^2 \backslash \mathcal{B}_{p_o,\rho}$, and by construction $\mathcal{N} \cap \mathcal{O} = \emptyset$, i.e., the obstacle \mathcal{N} does not intersect any of the sets \mathcal{O}_i , and the source set \mathcal{A}_J belongs to $\mathcal{O}_1 \cap \mathcal{O}_2$. This construction is always possible under minimal information of the position of the source. As an illustration, the sets \mathcal{O}_1 and \mathcal{O}_2 are shown in Figures 4 and 5 for the case when $p_0 = [1,0]^{\top}$ and $\rho = 0.1$.

Using this construction, a *model-free* source seeking controller will be designed to avoid the set $\mathcal{B}_{p_0,\rho}$ that contains the obstacle \mathcal{N} , from every initial condition not in $\mathcal{B}_{p_0,\rho}$.

B. Hybrid Localization Function

In order to find the source of the potential field J, we endow the control system of the vehicle with a logic state $q \in \{1,2\}$, that indicates which virtual set \mathcal{O}_q is currently being used by the controller. For each $q \in \{1,2\}$, we consider localization functions defined as follows:

$$V_q(p) := \begin{cases} J_q(p) - \hat{J}(p), & \forall \ p \in \mathcal{O}_q, \\ \infty, & \forall \ p \notin \mathcal{O}_q, \end{cases}$$
 (15)

where \hat{J} is the vehicle's *measurement* of the intensity of the potential field J, and where J_q is a virtual barrier signal defined only on each set \mathcal{O}_q . We consider localization functions V_q that satisfy the following assumption:

Assumption 4: Let $W_q := V_q + J^*$. The hybrid localization functions $\{V_q\}_{q \in \{1,2\}}$ satisfy:

(a) For each $q \in \{1, 2\}$ there exist functions $\alpha_{1,q}, \alpha_{2,q} \in \mathcal{K}_{\infty}$, and proper indicators $\tilde{\omega}_q$ of \mathcal{A}_J on \mathcal{O}_q , such that

$$\alpha_{1,q}(\tilde{\omega}_q(p)) \le W_q(p) \le \alpha_{2,q}(\tilde{\omega}_q(p)), \quad \forall \ p \in \mathcal{O}_q.$$

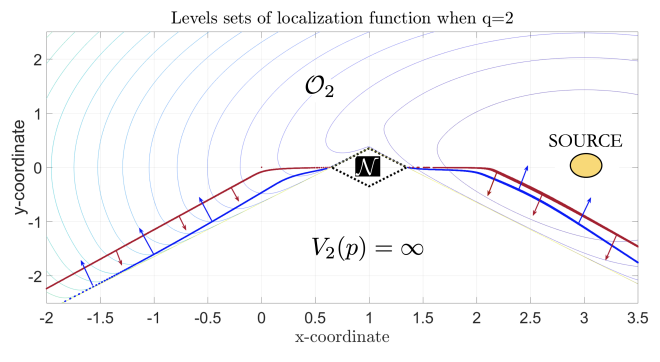


Fig. 5: Space \mathcal{O}_q with q=2. The blue arrows indicate the flow set (18a) and the red arrows indicate the jump set (18b). The box contains $\mathcal{B}_{p_0,\rho}$.

(b) For each $q \in \{1, 2\}$, we have

$$\mathcal{Z}_{\nabla W_q} = \{ p^* \in \mathcal{O}_q : \nabla W_q(p^*) = 0 \} = \mathcal{A}_J,$$

where A_J is given by Assumption 1.

(c) For each $q \in \{1,2\}$, the function $V_q(\cdot)$ is continuously differentiable in \mathcal{O}_q .

Note that for each $q \in \{1,2\}$, we have $\nabla W_q = \nabla V_q$, and by item (b) in Assumption 4 the set of minima of the localization function (15) is consistent with the source set \mathcal{A}_J , even though the signal \hat{J} may be different from the original potential field. In general, the condition $\mathcal{Z}_{\nabla W_q} = \mathcal{A}_J$ also implies that W_q is not a global navigation function [17], since any critical point of ∇W_q must be a global minima. However, unlike standard approaches based on navigation functions [9], [21], the conditions in Assumption 4 need to be checked only on the set \mathcal{O}_q . For the case when $\hat{J} = J$, under Assumption 1 the construction of the barrier function J_q can be easily carried out for some classes of potential fields [24], [36]. A typical case corresponds to quadratic potentials, which are ubiquitous in source-seeking problems; see [6], [8]–[10], [31].

Example 2 (Example 1 continued): For a quadratic potential field such as the one in Example 1, we can construct J_q as $J_q(p) := B(\tilde{d}_q(p))$, where $\tilde{d}_q(p) := |p|^2_{\mathbb{R}^2 \setminus \mathcal{O}_q}$, and

$$B(s) := \begin{cases} (s - \rho)^2 \log\left(\frac{1}{s}\right), & \text{if } s \in [0, \rho] \\ 0, & \text{if } s > \rho, \end{cases}$$
 (16)

with $\rho \in (0,1]$ being a tunable parameter selected sufficiently small. Under Assumption 1, for each fixed q the resulting localization function V_q is continuously differentiable in \mathcal{O}_q . Also, $V_q \to \infty$ as $p \to \mathbb{R}^2 \backslash \mathcal{O}_q$ or $|p| \to \infty$. Moreover, item (b) of Assumption 4 is also satisfied as shown in Figures 4 and 5, which show the level sets of the resulting localization functions V_1 and V_2 constructed as in (15).

C. Hybrid Source Seeking Dynamics

Once the operational space of the vehicle has been covered by the set $\mathcal{O}_1 \cup \mathcal{O}_2$, and a family of localization functions has been defined, we consider the following adaptive hybrid source seeking dynamics

$$u := -\mathcal{F}_a(p)\mu, \quad \mathcal{F}_a(p) := -a\omega R + 2ka^{-1}V_a(p)I_{2\times 2}, \quad (17)$$

where $[k,a,\omega]^{\top}\in\mathbb{R}^3_{>0}$ are again tunable parameters, $q\in\{1,2\}$ is a switching logic state, and where μ is a dither signal generated by the oscillator dynamics in (5). To characterize the switching behavior of the controller, consider the sets

$$\begin{split} C_{p,q} &:= \left\{ (p,q) \in \overline{\mathcal{O}} \times \{1,2\} : V_q(p) \leq \chi V_{3-q}(p) \right\}, \ \ \text{(18a)} \\ D_{p,q} &:= \left\{ (p,q) \in \overline{\mathcal{O}} \times \{1,2\} : V_q(p) \geq (\chi - \lambda) V_{3-q}(p) \right\}, \\ \text{(18b)} \end{split}$$

where $\chi \in (1, \infty)$ and $\lambda \in (0, \chi - 1)$ are tunable parameters. Note that the term $(\chi - \lambda)$ in (18b) guarantees that the intersection of the sets $C_{p,q}$ and $D_{p,q}$ is not empty. The set $C_{p,q}$ characterizes the points in the space $\overline{\mathcal{O}} \times \{1,2\}$ where the vehicle implements the adaptive navigation law (17) with constant state q, i.e., with $\dot{q} = 0$. On the other hand, the set $D_{p,q}$ characterizes the points in the space $\overline{\mathcal{O}} \times \{1,2\}$ where the vehicle toggles its logic state q as $q^+ = 3 - q$. Since by construction $\chi > 1$ and $\chi - \lambda > 1$, the vehicle toggles the potential field V_q whenever its current value exceeds a threshold compared to the other potential field V_{3-a} . After switching the controller, the vehicle will flow again using the new potential field V_{3-q} , until a new jump (if at all) is triggered by approaching points in the space where the potential again exceeds a threshold involving V_q . This switching rule effectively imposes a hysteresis property in the controller.

Based on the previous construction, the closed-loop system is a HDS, with state $z = [p^{\top}, q, \mu^{\top},]^{\top} \in \mathbb{R}^5$, flows given by

$$\dot{z} = F_z(z) := \begin{bmatrix} -\mathcal{F}_q(p)\mu \\ 0 \\ \omega R\mu \end{bmatrix}, \quad z \in C_z := C_{p,q} \times \mathbb{S}^1, \quad (19)$$

and jumps given by

$$z^{+} = G_{z}(z) := \left[p^{\top}, 3 - q, \mu^{\top} \right]^{\top}, \ z \in D_{z} := D_{p,q} \times \mathbb{S}^{1}.$$
 (20)

By construction, this system satisfies the Basic Conditions (C1)-(C3).

Remark 1: In the obstacle-free case, existing smooth model-free dynamics can achieve source seeking without measurements of the position of the vehicle, e.g., [6], [31]. However, when there are obstacles, GPS-denied source seeking controllers based on navigation functions can achieve source seeking only from almost all initial conditions [9]. On the other hand, the hybrid adaptive dynamics (19)-(20) use continuous measurements of the intensity of the virtual functions J_q , which depend on the relative position of the vehicle with respect to the set \mathcal{O}_q . As shown in the next section, this extra level of information will be enough to guarantee suitable (semi) global (practical) stability and robustness properties for the closed-loop system.

D. Analysis

The HDS (19)-(20) can be analyzed by a nested application of singular perturbation theory [37], [38]:

1) Change of Variable and Nominal HDS: Consider the change of variable $\tilde{p}:=p-a\mu$ and the Taylor expansion (8) applied to the hybrid localization function V_q , which

transforms system (19)-(20) into a HDS with flows given by

$$\dot{\tilde{p}} = -2k\mu \left(\frac{V_q(\tilde{p})}{a} + \ \mu^\top \nabla V_q(\tilde{p}) \right) + e_V, \ \dot{q} = 0, \ \dot{\mu} = \omega R\mu,$$
(21)

which are allowed whenever $(\tilde{p} + e_p, q, \mu) \in C_z$. The jumps of the HDS are given by

$$\tilde{p}^+ = \tilde{p}, \quad q^+ = 3 - q, \quad \mu^+ = \mu, \quad (\tilde{p} + e_p, q, \mu) \in D_z.$$
 (22)

Here, the signals e_V and e_p are of order $\mathcal{O}(a)$.

2) Averaging Theory for Hybrid System: For values of ω^{-1} sufficiently small, the HDS (21)-(22) is a singularly perturbed HDS [39]. Consider the change of variable $\tau := \omega t$, which generates the same jumps (22), and the new flows in the τ -time scale, allowed when $(\tilde{p} + e_p, q, \mu) \in C_z$, and given by

$$\dot{\tilde{p}} = -2k\omega^{-1}\mu \left[\frac{V_q(\tilde{p})}{a} + \mu^\top \nabla V_q(\tilde{p}) + e_v \right], \ \dot{q} = 0, \ \dot{\mu} = R\mu.$$
(23)

The boundary layer system [39, Eq. (6)] is now obtained by taking $\omega^{-1} = 0$ in (23), and by ignoring the jumps (22):

$$\dot{\tilde{p}} = 0, \quad \dot{q} = 0, \quad \dot{\mu} = R\mu, \quad (\tilde{p} + e_p, q, \mu) \in C_z.$$
 (24)

By Lemma 2, for each compact set $K \subset \mathbb{R}^3$ and each $(p,q) \in C_{p,q} \cap K$, the solutions μ of (24) satisfy the orthogonality and zero-average properties. Substituting μ in (23) and taking the average of the right-hand side, we obtain the *average hybrid system* [39, Def. 5], which in the original time scale has flows:

$$\dot{\tilde{p}}^a = -k\nabla V_q(\tilde{p}^a) + \tilde{e}_V, \ \dot{q}^a = 0, \ (\tilde{p}^a + e_p, q^a) \in C_{p,q}, \ (25)$$

and jumps

$$\tilde{p}^{a,+} = \tilde{p}^a, \quad q^{a,+} = 3 - q^a, \quad (\tilde{p}^a + e_n, q^a) \in D_{n,q}, \quad (26)$$

where \tilde{e}_V and e_p are of order $\mathcal{O}(a)$, and therefore can be treated as small disturbances acting on a *nominal* HDS with $e_V = e_p = 0$.

3) Asymptotic Stability of the Nominal Average Hybrid System: We now show that the average HDS (25)-(26) with $e_V=e_p=0$ renders the set $\mathcal{A}_J\times\{1,2\}$ uniformly globally asymptotically stable with basin of attraction \mathcal{O} . Defining $\tilde{\omega}(\tilde{p}^a):=\min_{q^a\in Q}\sum_{s.t.}\tilde{p}^a\in\mathcal{O}_{q^a}\tilde{\omega}_{q^a}(\tilde{p}^a)$ for each $\tilde{p}^a\in\mathcal{O}$, we obtain that $\tilde{\omega}$ is a proper indicator of \mathcal{A}_J on \mathcal{O} . Also, taking $\alpha_1(s):=\min_{q^a\in Q}\alpha_{1,q^a}(s)$ and $\alpha_2(s):=\max_{q^a\in Q}\alpha_{2,q^a}(s)$, and using Assumption 4-(a) we obtain that

$$\alpha_1(\tilde{\omega}(\tilde{p}^a)) \le W_{q^a}(\tilde{p}^a) \le \alpha_2(\tilde{\omega}(\tilde{p}^a)), \quad \forall \ \tilde{p}^a \in \mathcal{O}.$$
 (27)

Moreover, during flows we have $\dot{W}_q(\tilde{p}^a) = \dot{V}_{q^a}(\tilde{p}^a)$ and

$$\dot{V}_{q^a}(\tilde{p}^a) = -k|\nabla V_{q^a}(\tilde{p}^a)|^2 < 0,$$

for all $(\tilde{p}^a,q^a)\in C_{p,q}\cap(\mathcal{O}\backslash\mathcal{A}_J)\times\{q\}$, which implies that, for each $q^a\in\{1,2\}$, the localization function $V_q(\tilde{p}^a)$ decreases outside the set \mathcal{A}_J . On the other hand, jumps are allowed only when the localization function V_{q^a} gets larger or equal than the localization function V_{3-q^a} multiplied by the factor $(\chi-\lambda)$, which, by construction, is greater than 1. Therefore, during jumps we have that

$$V_{q^{a,+}}(\tilde{p}^{a,+}) \le \frac{1}{\gamma - \lambda} V_{q^a}(\tilde{p}^a), \quad \forall \ (\tilde{p}^a, q^a) \in D_{p,q}.$$

Zeno solutions are avoided due to the hysteresis switching mechanism induced by the construction of the flow and jump set. Thus, the Lyapunov function $W(\tilde{p}^a, q^a)$ uniformly decreases along solutions guaranteeing uniform convergence of \tilde{p}^a to \mathcal{A}_J . Uniform asymptotic stability of $\mathcal{A}_J \times \{1,2\}$ with basin of attraction $\mathcal{O} \times \{1,2\} = \mathbb{R}^2 \setminus \mathcal{B}_{p_o,\rho} \times \{1,2\}$ follows now directly by [29, Prop.7.5].

4) Stability of the HDS (21)-(22): Since the set $A_J \times \{1,2\}$ is uniformly asymptotically stable for the average nominal system (25)-(26) with $e_V = e_p = 0$, by Lemma 1 the same set is SGPAS as $a \to 0^+$ for the $\mathcal{O}(a)$ -perturbed HDS (21)-(22). We can now apply averaging theory for perturbed HDS [40, Thm. 7] to directly conclude that the original dynamics (21)-(22) render the set $A_J \times \{1,2\} \times \mathbb{S}$ SGPAS as $(a,\omega^{-1}) \to 0^+$. Since the HDS satisfies the Hybrid Basic Conditions, robustness with respect to arbitrarily small adversarial jamming signal e follows directly by Lemma 1. Finally, obstacle avoidance follows by the forward invariance of the basin of attraction \mathcal{O} [29, Thm. 7.12], and the ε -closeness of solutions between (25)-(26) [39, Thm. 1], and \tilde{p} in (21)-(22).

We summarize with the following Theorem, which is the first main result of this paper.

Theorem 1: Suppose that Assumptions 1-4 hold and consider the HDS (19)-(20). For each compact set $K_0 \subset \mathbb{R}^2 \backslash \mathcal{B}_{p_o,\rho}$ and each $\varepsilon \in \mathbb{R}_{>0}$, there exists $a^* \in \mathbb{R}_{>0}$ such that for each $a \in (0,a^*)$ there exists $\omega^* \in \mathbb{R}_{>0}$ such that for each $\omega > \omega^*$ there exists $\delta^* \in \mathbb{R}_{>0}$ such that for each measurable perturbation $e: \mathrm{dom}(e) \to \delta \mathbb{B}$ with $\delta \in [0,\delta^*]$, each complete solution of the perturbed HDS

$$\dot{z} = F_z(z+e), \quad z+e \in C_z \tag{28a}$$

$$z^{+} = G_z(z+e), \quad z+e \in D_z,$$
 (28b)

with initial condition $p(0,0) \in K_0$ generates trajectories p that: a) converge to $\mathcal{A}_J + (\varepsilon + a)\mathbb{B}$ in finite time; b) satisfy $p(t,j) \notin \mathcal{N}$ for all $(t,j) \in \text{dom}(z)$. \diamondsuit

Remark 2: The result of Theorem 1, which is similar in spirit to other convergence results for averaging-based source seeking algorithms (with no obstacles), states that by orderly tuning the parameters of the controller, the trajectories of the vehicle achieve semi-global practical convergence to the source of the signal, while avoiding the obstacle, and subject to small additive disturbances e on the states and dynamics of the system.

V. COORDINATED SOURCE SEEKING AND OBSTACLE AVOIDANCE IN MULTI-VEHICLE SYSTEMS

In the previous section, we studied how to design robust hybrid source seeking dynamics for single-vehicle systems operating under obstacles and small disturbances *e* of arbitrary frequency. In this section, we now study how to design robust *cooperative coordinated* hybrid source seeking dynamics with obstacle avoidance for MVS.

A. Formation Specification and Cooperative Localization Functions

We consider MVS with communication networks characterized by unweighted time-invariant graphs $\mathcal{G} = \{\mathcal{V}, \mathcal{E}\}$ satisfying the following assumption.

Assumption 5: The graph \mathcal{G} is undirected and connected. \square Remark 3: We consider time-invariant undirected graphs mainly to simplify our presentation and to avoid auxiliary states and notation needed to model time-varying directed graphs. However, by following the ideas of [41, Sec. 6], our results could also be extended to directed graphs that are strongly connected "sufficiently often" in time.

To design the cooperative hybrid dynamics, we assume that the potential field J can only be sensed by a subset $S \subset \mathcal{V}$ of the vehicles. In order to model this scenario, we assign a pinning gain $\gamma_i \in \{0,1\}$ to each agent $i \in \mathcal{V}$. These parameters satisfy $\gamma_i = 1$ if and only if $i \in S$. The localization function of each agent is then defined as

$$V_{q_i}(p_i) := \begin{cases} J_{q_i}(p_i) - \gamma_i \hat{J}_i(p_i), & \forall \ p_i \in \mathcal{O}_{q_i}, \\ \infty, & \forall \ p_i \in \mathbb{R}^2 \backslash \mathcal{O}_{q_i}, \end{cases}$$
(29)

where again $q_i \in \{1, 2\}$ and the sets \mathcal{O}_1 and \mathcal{O}_2 are defined as in (14). In order to have coordinated source seeking in the multi-vehicle system, a particular formation is defined a priori. This formation is specified by the vector

$$p_f := [x_f^\top, y_f^\top]^\top \in \mathbb{R}^{2N}, \tag{30}$$

where $x_f := [x_{f,1}, x_{f,2}, \dots, x_{f,N}]^\top \in \mathbb{R}^N$ and $y_f := [y_{f,1}, y_{f,2}, \dots, y_{f,N}]^\top \in \mathbb{R}^N$, which contains the formation coordinates of each vehicle i, given by $p_{f,i} = [x_{f,i}, y_{f,i}]^\top \in \mathbb{R}^2$. We will work with *consistent* formations that are translationally invariant, which are standard in formation control problems; see [42, Sec. 6.1].

Definition 3: The multi-vehicle system with individual dynamics (2) is said to satisfy a consistent formation $p_f \in \mathbb{R}^{2N}$ if $p_{f,i} = \mathbf{0}_2$ for all $i \in S$, and there exists $\zeta = [\zeta_x, \zeta_y]^\top \in \mathbb{R}^2$ such that $p_i = p_{f,i} + \zeta$, for all $i \in \mathcal{V}$.

After introducing a particular consistent formation for the multi-vehicle system, we are now interested in steering the vehicles towards the compact set

$$\mathcal{A}_{\text{coord}} := \left\{ p \in \mathbb{R}^{2N} : p = (I_2 \otimes \mathbf{1}_N) \cdot p^* + p_f, \ p^* \in \mathcal{A}_J \right\},\tag{31}$$

where the set \mathcal{A}_J is defined as in Assumption 1. In order to obtain obstacle avoidance and robust convergence to (31), we characterize a family of feasible localization functions. Let $x := [x_1, \dots, x_N]^\top$, $y := [y_1, \dots, y_N]$, $p := [x^\top, y^\top]^\top$, $q := [q_1, \dots, q_N]^\top$, and consider the *cooperative* localization function

$$W_{\text{coop}}(p,q) = \sum_{i \in \mathcal{V}} V_{q_i}(p_i) + \frac{1}{2} (p - p_f)^{\top} (I_2 \otimes L) (p - p_f), \quad (32)$$

where L is the Laplacian matrix of the graph \mathcal{G} . The individual functions V_{q_i} are now designed to satisfy the following assumption.

Assumption 6: For the multi-vehicle system with cooperative localization function (32), the following holds:

(a) For each $q \in \{1,2\}^N$ there exists functions $\alpha_{1,q}, \alpha_{2,q} \in \mathcal{K}_{\infty}$, and proper indicators $\tilde{\omega}_q$ of $\mathcal{A}_{\text{coord}}$ on $\tilde{\mathcal{O}}_q := \mathcal{O}_{q_1} \times \mathcal{O}_{q_2} \times \ldots \times \mathcal{O}_{q_N}$, such that

$$\alpha_{1,q}(\tilde{\omega}_q(p)) \le W_{\text{coop}}(p,q) \le \alpha_{2,q}(\tilde{\omega}_q(p)), \quad \forall \ p \in \tilde{\mathcal{O}}_q.$$
(33)

(b) For each $q \in \{1, 2\}^N$, we have

$$\mathcal{Z}_{\nabla W_{\text{coop}}} = \left\{ \hat{p} \in \tilde{\mathcal{O}}_q : \nabla W_{\text{coop}}(\hat{p}, q) = 0 \right\} = \mathcal{A}_{\text{coord}}.$$

(c) For each $i \in \mathcal{V}$, the function $V_{q_i}(\cdot)$ is continuously differentiable in \mathcal{O}_{q_i} .

Remark 4: Given that our goal is to guarantee robust source seeking and obstacle avoidance in MVS from every possible compact set of initial conditions in the operational space of the vehicle, Assumption 6 leads to the verification of 2^N different conditions. If, on the other hand, the vehicles are initialized sufficiently close to each other such that they implement the same logic state q_i for all time, items (a) and (b) can be relaxed, and only N conditions (with a common q_i) need to be verified.

As in Assumption 4, the conditions of Assumption 6 can be satisfied in each set \mathcal{O}_q by consistent formations and suitable combinations of barrier functions and typical choices of potential fields, including, but not limited to, quadratic functions.

Example 3: (Examples 1 and 2 Continued) As in Examples 1 and 2, suppose that the seeking vehicles have access to individual measurements of a quadratic potential field of the form $\hat{J}_i(x_i, y_i) = -\frac{w_{x,i}}{2}(x_i - x^*)^2 - \frac{w_{y,i}^2}{2}(y_i - y^*)^2$, where $[w_{x,i}, w_{x,i}] \in \mathbb{R}^2_{>0}$. Using the change of variable $\tilde{p} = p - (I_2 \otimes I_2)$ $(\mathbf{1}_N) \cdot p^* - p^f$ and the facts that $L\mathbf{1}_N = \mathbf{0}$ and $\mathbf{1}_N^\top L = \mathbf{0}$ induced by Assumption 5, the cooperative localization function can be written as $W_{\text{coop}} = \sum_{i \in \mathcal{V}} J_{q_i}(\tilde{p}_i + p^* + p_{f,i}) + \frac{1}{2} \tilde{p}^\top T \tilde{p}$, where $T = [(I_2 \otimes L) + (I_2 \otimes I(\gamma))I(w)]$. Since $L = L^{\top}$ is positive semidefinite, kernel(L) = span{ $\mathbf{1}_N$ }, and $I(\gamma)I(w)$ is diagonal with at least one positive entry, we have that $\lambda_{min}(T) > 0$. Finally, using the family of barrier functions defined in (16), we obtain that each J_{q_i} is zero for all points p_i away from \mathcal{O}_{q_i} by at least ρ_i , and grows to ∞ as $p_i \to \mathrm{bd}(\mathcal{O}_{q_i}) \cup \{\infty\}$. In particular, Assumption 6 holds if $|p^* + p_{f_i}|_{\mathrm{bd}(\mathcal{O}_{q_i})} > \rho_i \text{ for all } i \in \mathcal{V}.$

B. Model-Free Hybrid Dynamics of the Multi-Vehicle System

As in the single-vehicle case, we now endow each vehicle with an individual excitation signal μ_i with frequency ω_i $\bar{\omega}\kappa_i$, tunable parameters $[\bar{\omega}, \kappa_i, a_i]^{\top} \in \mathbb{R}^3_{>0}$, and a logic state $q_i \in \{1, 2\}$, and for each vehicle we use the same geometric covering of the operational space as in Section IV-A. Using this covering, the feedback law for the multi-vehicle system is given by the cooperative adaptive hybrid controller

$$u_{coop} := -\mathcal{F}_q(p)(\mathbf{1}_2 \otimes \mu) - (I_2 \otimes I(k)L)\,\hat{p},\tag{34}$$

where $\hat{p} = p - p_f$, $\mu = [\mu_1^\top, \mu_2^\top, \dots, \mu_N^\top]^\top$, with mapping $\mathcal{F}_q(p) := \left[\mathcal{F}_{q,x}(p)^\top, \mathcal{F}_{q,y}(p)^\top \right]^\top$, where

$$\mathcal{F}_{q,x}(p) := \begin{bmatrix} \mathcal{F}_{q,x,1}(p_1) \\ \mathcal{F}_{q,x,2}(p_2) \\ \vdots \\ \mathcal{F}_{q,x,N}(p_N) \end{bmatrix}, \ \mathcal{F}_{q,y}(p) := \begin{bmatrix} \mathcal{F}_{q,y,1}(p_1) \\ \mathcal{F}_{q,y,2}(p_2) \\ \vdots \\ \mathcal{F}_{q,y,N}(p_N) \end{bmatrix}, \ \mathcal{F}_{q,y}(p) := \begin{bmatrix} \mathcal{F}_{q,y,1}(p_1) \\ \mathcal{F}_{q,y,2}(p_2) \\ \vdots \\ \mathcal{F}_{q,y,N}(p_N) \end{bmatrix}, \ \mathcal{F}_{q,y}(p) := \begin{bmatrix} \mathcal{F}_{q,y,1}(p_1) \\ \mathcal{F}_{q,y,2}(p_2) \\ \vdots \\ \mathcal{F}_{q,y,N}(p_N) \end{bmatrix}, \ \mathcal{F}_{q,y}(p) := \begin{bmatrix} \mathcal{F}_{q,y,1}(p_1) \\ \mathcal{F}_{q,y,2}(p_2) \\ \vdots \\ \mathcal{F}_{q,y,N}(p_N) \end{bmatrix}, \ \mathcal{F}_{q,y}(p) := \begin{bmatrix} \mathcal{F}_{q,y,1}(p_1) \\ \mathcal{F}_{q,y,2}(p_2) \\ \vdots \\ \mathcal{F}_{q,y,N}(p_N) \end{bmatrix}, \ \mathcal{F}_{q,y}(p) := \begin{bmatrix} \mathcal{F}_{q,y,1}(p_1) \\ \mathcal{F}_{q,y,2}(p_2) \\ \vdots \\ \mathcal{F}_{q,y,N}(p_N) \end{bmatrix}, \ \mathcal{F}_{q,y}(p) := \begin{bmatrix} \mathcal{F}_{q,y,1}(p_1) \\ \mathcal{F}_{q,y,2}(p_2) \\ \vdots \\ \mathcal{F}_{q,y,N}(p_N) \end{bmatrix}, \ \mathcal{F}_{q,y}(p) := \begin{bmatrix} \mathcal{F}_{q,y,1}(p_1) \\ \mathcal{F}_{q,y,2}(p_2) \\ \vdots \\ \mathcal{F}_{q,y,N}(p_N) \end{bmatrix}, \ \mathcal{F}_{q,y}(p) := \begin{bmatrix} \mathcal{F}_{q,y,1}(p_1) \\ \mathcal{F}_{q,y,1}(p_2) \\ \vdots \\ \mathcal{F}_{q,y,N}(p_N) \end{bmatrix}, \ \mathcal{F}_{q,y}(p) := \begin{bmatrix} \mathcal{F}_{q,y,1}(p_1) \\ \mathcal{F}_{q,y,1}(p_2) \\ \vdots \\ \mathcal{F}_{q,y,N}(p_N) \end{bmatrix}, \ \mathcal{F}_{q,y}(p) := \begin{bmatrix} \mathcal{F}_{q,y,1}(p_1) \\ \mathcal{F}_{q,y,1}(p_2) \\ \vdots \\ \mathcal{F}_{q,y,N}(p_N) \end{bmatrix}, \ \mathcal{F}_{q,y}(p) := \begin{bmatrix} \mathcal{F}_{q,y,1}(p_1) \\ \mathcal{F}_{q,y,1}(p_2) \\ \vdots \\ \mathcal{F}_{q,y,N}(p_N) \end{bmatrix}, \ \mathcal{F}_{q,y}(p) := \begin{bmatrix} \mathcal{F}_{q,y,1}(p_1) \\ \mathcal{F}_{q,y,1}(p_2) \\ \vdots \\ \mathcal{F}_{q,y,N}(p_N) \end{bmatrix}, \ \mathcal{F}_{q,y}(p) := \begin{bmatrix} \mathcal{F}_{q,y,1}(p_1) \\ \mathcal{F}_{q,y,1}(p_2) \\ \vdots \\ \mathcal{F}_{q,y,N}(p_N) \end{bmatrix}, \ \mathcal{F}_{q,y}(p) := \begin{bmatrix} \mathcal{F}_{q,y,1}(p_1) \\ \mathcal{F}_{q,y,1}(p_2) \\ \vdots \\ \mathcal{F}_{q,y,N}(p_N) \end{bmatrix}, \ \mathcal{F}_{q,y}(p) := \begin{bmatrix} \mathcal{F}_{q,y,1}(p_1) \\ \mathcal{F}_{q,y,1}(p_2) \\ \vdots \\ \mathcal{F}_{q,y,N}(p_N) \end{bmatrix}, \ \mathcal{F}_{q,y}(p) := \begin{bmatrix} \mathcal{F}_{q,y,1}(p_1) \\ \mathcal{F}_{q,y,1}(p_2) \\ \vdots \\ \mathcal{F}_{q,y,N}(p_N) \end{bmatrix}, \ \mathcal{F}_{q,y}(p) := \begin{bmatrix} \mathcal{F}_{q,y,1}(p_1) \\ \mathcal{F}_{q,y,1}(p_2) \\ \vdots \\ \mathcal{F}_{q,y,N}(p_N) \end{bmatrix}, \ \mathcal{F}_{q,y}(p) := \begin{bmatrix} \mathcal{F}_{q,y,1}(p_1) \\ \mathcal{F}_{q,y,1}(p_2) \\ \vdots \\ \mathcal{F}_{q,y,N}(p_N) \end{bmatrix}, \ \mathcal{F}_{q,y}(p) := \begin{bmatrix} \mathcal{F}_{q,y,1}(p_1) \\ \mathcal{F}_{q,y,1}(p_2) \\ \vdots \\ \mathcal{F}_{q,y,N}(p_N) \end{bmatrix}, \ \mathcal{F}_{q,y}(p) := \begin{bmatrix} \mathcal{F}_{q,y,1}(p_1) \\ \mathcal{F}_{q,y,1}(p_2) \\ \vdots \\ \mathcal{F}_{q,y,N}(p_N) \end{bmatrix}, \ \mathcal{F}_{q,y}(p) := \begin{bmatrix} \mathcal{F}_{q,y,1}(p_1) \\ \mathcal{F}_{q,y}(p_1) \\ \vdots \\ \mathcal{F}_{q,y,N}(p_N) \end{bmatrix}$$

$$\begin{bmatrix} \mathcal{F}_{q,x,i} \\ \mathcal{F}_{q,y,i} \end{bmatrix} := -a_i \omega_i R + 2k_i a_i^{-1} V_{q_i}(p_i) I_{2 \times 2}.$$

The continuous-time dynamics of the individual logic states and excitation signals of the vehicles are still given by $\dot{q}_i = 0$ and $\dot{\mu}_i = \omega_i R \mu_i$, with $\mu_i \in \mathbb{S}^1$ and $q_i \in \{1, 2\}$. The discretetime dynamics are given by $p_i^+ = p_i$, $q_i^+ = 3 - q_i$, and $\mu_i^+ =$ μ_i . For each $(\chi_i, \lambda_i) \in (1, \infty) \times (0, \chi_i - 1)$ the individual sets that characterize the switching rule of the logic state q_i of each vehicle are given by

$$C_{p,q}^{i} := \left\{ (p_{i}, q_{i}) \in \overline{\mathcal{O}} \times \{1, 2\} : V_{q_{i}}(p_{i}) \le \chi_{i} V_{3-q_{i}}(p_{i}) \right\},$$
(35a)

$$D_{p,q}^i := \left\{ (p_i, q_i) \in \overline{\mathcal{O}} \times \{1, 2\} : \right.$$

$$V_{q_i}(p_i) \ge (\chi_i - \lambda_i) V_{3-q_i}(p_i)$$
. (35b)

As in the single-vehicle case, the feedback law (34) and the evaluation of the sets (35) are model-free.

Remark 5: In the control law (34), we allow each vehicle to use exploratory signals irrespective of their roles as leaders or followers. This allows the followers to use realtime measurements of the localization functions V_{q_i} instead of pre-computed gradients of barrier functions. However, if such virtual gradients are available, the followers can dispense with the exploratory signals by setting $a_i = 1$ and $\omega_i = 0$, and using ∇J_{q_i} instead of V_{q_i} .

C. Hybrid Systems Modeling

The analysis of the coordinated hybrid source seeking controller is more complicated due to the fact that several jumps can simultaneously occur in the system. Indeed, the overall dynamics correspond to a HDS with state $z = [p^{\top}, q^{\top}, \mu^{\top}]^{\top}$, and continuous-time dynamics

$$\dot{z} = F_{coop}(z) := \begin{bmatrix} -\mathcal{F}_q(p) \left(\mathbf{1}_2 \otimes \mu \right) - \left(I_2 \otimes I(k) \mathbf{L} \right) \hat{p} \\ \mathbf{0}_N \\ \left(I(\omega) \otimes R \right) \mu \end{bmatrix},$$
(36)

with $k := [k_1, ..., k_N]^{\top}$, $a := [a_1, ..., a_N]^{\top}$, and $\omega :=$ $[\omega_1,\ldots,\omega_N]^{\top}$. These flows capture the dynamics of the multivehicle system whenever the state z is in the flow set

$$C_{coop} := \left\{ z \in \mathcal{O}^N \times \{1, 2\}^N \times \mathbb{S}^N : (p, q) \in \tilde{C}_{p, q}^N \right\}, (37)$$

where $\tilde{C}_{p,q}^N:=C_{p,q}^1\times C_{p,q}^2\times\ldots\times C_{p,q}^N$. To model the discrete-time dynamics of the closed-loop system, consider the set

$$D_o := \left\{ z \in \mathcal{O}^N \times \{1, 2\}^N \times \mathbb{S}^N : \right.$$

$$(p_i, q_i) \in D^i_{p, q} \text{ for one and only one } i \in \mathcal{V} \right\}. (38)$$

The jumps of the system are then captured by the outer semicontinuous hull $\overline{G}_{\text{coop}}$ of a mapping $G_{\text{coop}}: \mathbb{R}^{2N} \times \{1,2\}^N \times \mathbb{S}^N \rightrightarrows \mathbb{R}^{2N} \times \{1,2\}^N \times \mathbb{S}^N$ that is non-empty only

$$G_{\text{coop}}(z) := [p^\top, Q(q)^\top, \mu^\top]^\top,$$

where $Q(q) = q - I(e_i)(3 - 2q)$. The complete jumps of the hybrid system are then given by

$$z^+ \in \overline{G}_{\text{coop}}(z), \quad z \in D_{\text{coop}}.$$
 (39)

10

$$D_{\text{coop}} := \left\{ z \in \mathcal{O}^N \times \{1, 2\}^N \times \mathbb{S}^N : \right.$$

$$(p_i, q_i) \in D^i_{p,q}, \text{ for at least one } i \in \mathcal{V} \right\}.$$
 (40)

By construction, the HDS with flow map (36), flow set (37), jump map (39), and jump set (40), satisfies the Basic Conditions (C1)-(C3). Note that this system can generate non unique solutions whenever multiple vehicles i simultaneously satisfy $(p_i,q_i) \in D^i_{p,q}$. However, in this case at most N consecutive jumps can occur in the system.

D. Stability Analysis

To analyze the stability properties of the closed-loop system, consider the change of variable $\tilde{p}=p-I_2\otimes I(a)\tilde{\mu}$, where $\tilde{\mu}=[\mu_1^\top,\mu_2^\top],\ \mu_1=[\mu_{1,1},\mu_{2,1},\dots,\mu_{N,1}]^\top$, and $\mu_2=[\mu_{1,2},\mu_{2,2},\dots,\mu_{N,2}]^\top$. Using the Taylor expansion (8) for each localization function V_{q_i} , we obtain the continuous-time dynamics $\dot{q}=\mathbf{0}_N$, and

$$\begin{split} \dot{\tilde{p}} &= - \Big[\Lambda + (I_2 \otimes I(k) \mathsf{L}) \left(\tilde{p} - p_f + e_p \right) \Big], \ \dot{\mu} = \bar{\omega} \left(I(\kappa) \otimes R \right) \mu, \\ \text{with } \Lambda &:= 2 \left(I_2 \otimes \left[\hat{V} (\tilde{p} + I_2 \otimes I(a) \tilde{\mu}, q) \right] \right) \mu, \ \text{where} \ \hat{V} (\tilde{p} + I_2 \otimes I(a) \tilde{\mu}, q) \\ I_2 \otimes I(a) \tilde{\mu}, q) \ \text{is a vector with entries given by} \end{split}$$

$$\hat{V}_{i}(\tilde{p}_{i} + a_{i}\mu_{i}, q_{i}) = \frac{k_{i}}{a_{i}}V_{q_{i}}(\tilde{p}_{i}) + k_{i}\mu_{i}^{\top}\nabla V_{q_{i}}(\tilde{p}_{i}) + e_{V_{q}}, \quad (42)$$

where the terms e_p and e_{V_q} are of order $\mathcal{O}(a)$. Since $p^+ = p$ and $\mu^+ = \mu$ during jumps, the jump map is still given by

$$(\tilde{p}, q, \mu)^+ \in \overline{G}_{\text{coord}}(\tilde{p}, q, \mu),$$
 (43)

and the flow and jump sets are

$$\begin{split} \tilde{C} := \Big\{ (\tilde{p} + e_p, q, \mu) \in \mathcal{O}^N \times \{1, 2\}^N \times \mathbb{S}^N : \\ (\tilde{p} + e_p, q) \in \tilde{C}^N \Big\}, \end{aligned} \tag{44a} \\ \tilde{D} := \Big\{ (\tilde{p} + e_p, \ q, \mu) \in \mathcal{O}^N \times \{1, 2\}^N \times \mathbb{S}^N : \\ (\tilde{p}_i + e_{p,i}, q_i) \in D^i_{p,q}, \text{ for at least one } i \in \mathcal{V} \Big\}. \tag{44b} \end{split}$$

As in the previous section, we will analyze this system using averaging theory for hybrid dynamical systems.

1) Analysis via Averaging Theory: For values of $\frac{1}{\overline{\omega}}$ sufficiently small, the hybrid system (41), (43), (44) is in singular perturbation form. Considering the new time scale given by $\tau = \omega t$, we obtain the flows $\dot{q} = \mathbf{0}_N$, $\dot{\mu} = (I(\kappa) \otimes R) \mu$, and

$$\dot{\tilde{p}} = -\frac{1}{\bar{\omega}} \left(\Lambda + \left(I_2 \otimes I(k) L \right) \left(\tilde{p} - p_f \right) \right).$$

By setting $\frac{1}{\bar{\omega}}=0$, the boundary layer system, which ignores the jumps, is again given by $\dot{\tilde{p}}=0$ and $\dot{\mu}=(I(\kappa)\otimes R)\,\mu$, with flow set (44a). Since the dynamics of the states μ_i are decoupled, this system generates N signals $\mu_i:\mathbb{R}_{\geq 0}\to \mathbb{S}^1$ satisfying the orthogonality and zero-average conditions of Lemma 2. By averaging the dynamics of \tilde{p} along the solutions of μ , the first term of (42) vanishes and we obtain the average

hybrid system with state (\tilde{p}^a, q^a) and flows in the original time scale, given by $\dot{q}^a = \mathbf{0}_N$ and

$$\begin{split} \dot{\tilde{p}}^a &= -\left(I_2 \otimes I(k)\right) \left(\nabla V(\tilde{p}^a,q^a) + \left(I_2 \otimes \mathsf{L}\right) \left(\tilde{p}^a - p_f\right)\right) + e_v, \\ \text{(45)} \\ \text{where } e_v \text{ is of order } \mathcal{O}(a), \nabla V(\tilde{p}^a,q^a) &:= \left[\nabla V_{q^a,\tilde{x}}, \nabla V_{q^a,\tilde{y}}\right]^\top, \\ \nabla V_{q,\tilde{x}} &:= \left[\frac{\partial V_{q_1}}{\partial \tilde{x}_1^a}, \ldots, \frac{\partial V_{q_N}}{\partial \tilde{x}_N^a}\right], \text{ and } \nabla V_{q,\tilde{y}} &:= \left[\frac{\partial V_{q_1}}{\partial \tilde{y}_1^a}, \ldots, \frac{\partial V_{q_N}}{\partial \tilde{y}_N^a}\right]. \\ \text{The jumps of the average system are} \end{split}$$

$$(\tilde{p}^a, q^a)^+ \in \{(v_1, v_2) : (v_1, v_2, v_3) \in \overline{G}_{\text{coop}}(\tilde{p}^a, q^a, \mu), \mu \in \mathbb{S}^N \},$$
(46)

and the flow and jump sets of the average system are

$$C^{a} := \left\{ (\tilde{p}^{a} + e_{p}, q^{a}) \in \mathcal{O}^{N} \times \{1, 2\}^{N} : (\tilde{p}^{a}, q^{a}) \in \tilde{C}^{N} \right\}, \tag{47a}$$

$$D^a := \left\{ (\tilde{p}^a + e_p, \ q^a) \in \mathcal{O}^N \times \{1, 2\}^N : \right.$$
$$(\tilde{p}^a_i, q^a_i) \in D^i_{p, q}, \text{ for at least one } i \in \mathcal{V} \right\}. \tag{47b}$$

2) Lyapunov-based Analysis for the Average-Slow System: We now analyze the stability properties of the nominal average-slow HDS (45), (46), (47) with $e_v = e_p = 0$. In order to do this, we consider the Lyapunov-like function $W_{coop}(\tilde{p}^a,q^a)$ given by (32). For each $q\in\{1,2\}^N$, the derivative of W_{coop} along the solutions of (45) is given by $\dot{W} = -\nabla W(\tilde{p}^a,q^a)^{\top} [I_2\otimes I(k)] \nabla W(\tilde{p}^a,q^a)$, which, under Assumption 6 is negative definite with respect to the set \mathcal{A}_{coord} .

On the other hand, whenever an agent triggers a jump, we necessarily have again that $V_{q_i^+}(\tilde{p}_i^{a,+}) \leq \frac{55}{\chi_i - \lambda_i} V_{q_i}(\tilde{p}_i)$, and since the jump rule (46) does not change the position \tilde{p}_i of agent i, the second term of W_{coop} remains constant. Thus, during jumps we also have that $W(\tilde{p}^a, q^a)$ decreases. By the bounds (33), we obtain uniform convergence of (\tilde{p}^a, q^a) to the set $\mathcal{A}_{\text{coord}} \times \{1,2\}^N$. Positive invariance of $\mathcal{A}_{\text{coord}} \times \{1,2\}^N$ follows directly by construction. Thus, for the average hybrid system we obtain uniform asymptotic stability of the set $\mathcal{A}_{\operatorname{coord}} \times \{1,2\}^N$ with basin of attraction $\mathcal{O}^N \times \{1,2\}^N$. Again, since $\mathcal{O}^N = \mathbb{R}^{2N} \setminus \mathcal{B}^N_{p_0,\rho}$, the compact set of initial conditions in \mathcal{O}^N that does not include the obstacle can be taken arbitrarily large. Finally, since by construction of the flow and jump sets we have that $(\tilde{p}_i^a,q_i^a)\in C^i_{p,q}\backslash D^i_{p,q}$ holds after the $i^{t\hat{h}}$ vehicle jumps, there can be at most Nconsecutive jumps in the closed-loop system before the system starts to flow again, ruling out discrete-time solutions and Zeno behavior.

3) Stability of the Original System: Having established asymptotic stability of the set $\mathcal{A}_{\text{coord}} \times \{1,2\}^N$ for the nomimal average system (45)-(47), we can follow now the exact same argument as in Section IV-D using first Lemma 1, and then averaging theory for perturbed hybrid systems [40, Thm. 7]. We summarize with the following Theorem, which is the second main result of this paper.

Theorem 2: Suppose that Assumptions 1-6 hold. For each compact set $K_0 \subset \mathbb{R}^{2N} \backslash \mathcal{B}^N_{p_o,\rho}$ and each $\varepsilon \in \mathbb{R}_{>0}$, there exists $a^* \in \mathbb{R}_{>0}$ such that for each $a \in \mathbb{R}^N$ with $a_i \in (0,a^*)$ there exists $\bar{\omega}^* \in \mathbb{R}_{>0}$ such that for each $\bar{\omega} > \bar{\omega}^*$ there exists a $\delta^* \in \mathbb{R}_{>0}$ such that for each measurable perturbation $e: \mathrm{dom}(e) \to \delta \mathbb{B}$ with $\delta \in [0,\delta^*]$, each complete solution of the

perturbed system

$$\dot{z} = F_{\text{coop}}(z+e), \quad z+e \in C_{\text{coop}}$$
 (48a)

$$z^{+} = G_{\text{coop}}(z+e), \quad z+e \in D_{\text{coop}}, \tag{48b}$$

with $p(0,0) \in K_0$ generate trajectories p that: a) converge to $\mathcal{A}_{\text{coord}} + (\varepsilon + a)\mathbb{B}$ in finite time; b) satisfy $p_i(t,j) \notin \mathcal{N}$, for all $i \in \mathcal{V}$ and for all $(t,j) \in \text{dom}(z)$. \diamondsuit

As shown in the previous analysis, the model-free hybrid cooperative source seeking dynamics actually render the set $\mathcal{A}_{\text{coord}}$ SGPAS as $(a,\omega^{-1}) \to 0^+$, while achieving obstacle avoidance. One can interpret the family of cooperative localization functions $\{W_{p,q}\}$ as a class of *synergistic cooperative Lyapunov functions* that incorporate the sparsity properties of the graph \mathcal{G} . By using the hysteresis-based switching rule and the covering of the operational space of the vehicles, the distributed hybrid controllers are able to robustly and simultaneously achieve (semi) global (practical) obstacle avoidance, model-free source seeking, and formation control.

VI. Nonholonomic Models and Other Kinematic Dynamics

In this section, we extend our previous results to mobile robots evolving on the plane under more complicated kinematic models. To simplify our presentation, we focus on single-vehicle systems. In particular, we consider vehicles with continuous-time models with state $\gamma = [p^\top, \eta^\top]^\top \in \mathbb{R}^{2+\kappa}$ and dynamics of the form

$$\dot{\gamma} \in f_{\gamma}(\gamma, r), \quad \gamma \in \mathbb{R}^2 \times \Theta,$$
 (49)

where $\Theta \subset \mathbb{R}^{\kappa}$ is a compact set, $f_{\gamma} : \mathbb{R}^{2+\kappa} \times \mathbb{R}^2 \rightrightarrows \mathbb{R}^{2+\kappa}$ is an outer semicontinuous, locally bounded and convex-valued set-valued mapping, and r is the input or control action. The state η can be used to model auxiliary variables such as velocities, accelerations, angles, etc. Several models of vehicles can be captured by this setting, including smooth single-valued models such as the velocity-actuated point mass model (2), force-actuated point mass model [6], unicycles, and other nonholonomic systems; see [31]. Discontinuous models can also be written as (49) by considering their Krasovskii regularization; see [29, Ch. 4].

In order to achieve source seeking and obstacle avoidance in systems of the form (49), we will follow a multi-time scale approach, where a low level controller will robustly and globally stabilize (49) with respect to a particular external reference u, which, in turn, will be slowly controlled by the hybrid source seeking law studied in the previous section. While this multi-time scale approach has been studied before in the context of *smooth* extremum seeking [5], the novelty of our approach lies on the incorporation of hybrid seeking dynamics with *hybrid* internal fast controllers that allows us to robustly stabilize systems that may not be stabilizable by smooth feedback laws.

A. Mobile Robots Stabilizable by Hybrid Feedback

For nonlinear systems under geometric constraints, e.g., nonholonomic systems, it may be impossible to find a continuous or discontinuous time-invariant feedback law that achieves

robust global stabilization [19]. Therefore, in this section we consider mobile robots (49) that satisfy the following assumption.

Assumption 7: There exists a hybrid controller $\mathcal{H}_h:=\{\Psi_D^h,F_h,\Psi_D^h,G_h\}$ with internal state $h\in\mathbb{R}^\ell$, output $r:\mathbb{R}^{2+\kappa}\times\mathbb{R}^\ell\to\mathbb{R}^2$, and input $u\in\mathbb{R}^2$, such that for each $\rho>0$ the system

$$\begin{bmatrix} \dot{u} \\ \dot{\gamma} \\ \dot{h} \end{bmatrix} \in \begin{bmatrix} 0 \\ f_{\gamma}(\gamma, r(\gamma, h)) \\ F_{h}(h, u) \end{bmatrix}, (u, (\gamma, h)) \in \mathbb{R}^{2} \times \Psi_{C}^{h}(u),$$
(50a)

$$\begin{bmatrix} u^{+} \\ \gamma^{+} \\ h^{+} \end{bmatrix} \in \begin{bmatrix} u \\ \gamma \\ G_{h}(h, u) \end{bmatrix}, (u, (\gamma, h)) \in \mathbb{R}^{2} \times \Psi_{D}^{h}(u),$$
(50b)

satisfies the Basic Conditions (C1), (C2), and (C3), and there exist a compact set $\mathcal{T} \subset \mathbb{R}^{\ell}$ such that system (50) with restricted input $u \in \rho \mathbb{B}$ renders UGAS the set

$$\mathcal{M}_{\rho} = \left\{ (u, \gamma, h) : u \in \rho \mathbb{B}, p = u, \eta \in \Theta, h \in \mathcal{T} \right\}, \quad (51)$$

and no complete solution of (50) is purely discrete. \Box

A particular class of systems that satisfy Assumption 7, and which are relevant in the source seeking literature, are unicycles.

B. Hybrid Stabilization of the Unicycle

The classic unicycle has dynamics $\dot{x} = \cos(\theta)v$, $\dot{y} = \sin(\theta)v$, $\dot{\theta} = w$, where θ is the angle, v is the linear velocity, and w is the angular velocity. This system can also be written as follows; see [43]:

$$\dot{p} = \eta v, \quad \dot{\eta} = -wR\eta, \tag{52}$$

where $p = [x,y]^{\top}$ denotes the position in the plane, $\eta \in \mathbb{S}^1$ denotes the orientation of the vehicle, and R was defined in (4). While different existing controllers can stabilize the position of a unicycle; e.g., [12], [44], it is well-known that there is no smooth time-invariant continuous-time feedback controller that can achieve robust global stabilization of a reference point in position and orientation $\gamma^* = [p^*, \eta^*]^{\top} \in \mathbb{R}^2 \times \mathbb{S}^1$; see [45]. On the other hand, we can construct a hybrid feedback controller that achieves this task [27]. To do this, for each fixed reference p^* , we define the error coordinates $\tilde{p} = p - p^*$, which satisfy $\dot{\tilde{p}} = \dot{p} = \eta v$. We consider the linear velocity feedback law

$$v := -\rho_v(\tilde{p}^\top \eta), \tag{53}$$

where the function $\rho_v(\cdot)$ is continuous and defined such that $s\rho_v(s)>0$ for all $s\neq 0$ and $\rho_v(0)=0$. Using the energy function $V_v=0.5\tilde{p}^2$ we have that $\dot{V}_v=-\tilde{p}^\top\eta\cdot\rho_v(\tilde{p}^\top\eta)<0$, for all (\tilde{p},η) such that $\tilde{p}^\top\eta\neq 0$. This specifies a linear velocity controller that guarantees a decrease of \tilde{p} during flows, except when $\tilde{p}^\top\eta=0$. On the other hand, the angular velocity w will be controlled by a hybrid supervisor control system that switches between two controllers \mathcal{H}_1 and \mathcal{H}_2 designed to robustly track the reference signals $\eta_1^*:=-\frac{\tilde{p}}{|\tilde{p}|}$

and $\eta_2^* := \begin{bmatrix} \cos(\sigma(\tilde{p})\zeta_2) & -\sin(\sigma(\tilde{p})\zeta_2) \\ \sin(\sigma(\tilde{p})\zeta_2) & \cos(\sigma(\tilde{p})\zeta_2) \end{bmatrix} \eta^*$, respectively, where $\sigma(\cdot)$ is a C^2 function that is positive definite, and where the auxiliary state ζ_2 is generated by the oscillator $\dot{\zeta}_2 = -\alpha R \zeta_2, \ \zeta_2 \in \mathbb{S}^1$. The controllers \mathcal{H}_1 and \mathcal{H}_2 for global robust tracking in \mathbb{S}^1 need to be hybrid since it is impossible to robustly and globally stabilize a point in \mathbb{S}^1 using a time-invariant continuous (or discontinuous) feedback law. By combining the ideas of [43, pp. 4688] and [46, Ex. 35], these hybrid tracking controllers can be constructed as follows:

Step 1. Coordinate Transformation: Note that $x \ominus e_1 = x =$ $e_1 \oplus x$ for any vector $x \in \mathbb{R}^2$. Similarly, if $x \in \mathbb{S}^1$, then $x \ominus x^c = e_1 = x^c \ominus x$. We proceed to parameterize each tracking controller by a logic state $s \in \Omega := \{1, 2\}$, where s=1 corresponds to global tracking of η_1^* using \mathcal{H}_1 , and s=2 corresponds to global tracking of η_2^* using \mathcal{H}_2 . We use $\eta_{s,j}^*$ to denote the j^{th} component of η_s^* , with $j \in \{1,2\}$. Based on this, we consider the coordinate transformation $\eta = \tilde{\eta}_s \ominus \eta_s^*$ where $\tilde{\eta}_s \in \mathbb{R}^2$. This transformation implies that $\eta \ominus \eta_s^{*c} =$ $\tilde{\eta}_s\ominus\eta_s^*\ominus\eta_s^{*c}=\tilde{\eta}_s\in\mathbb{S}^1$. Moreover, note that if $\tilde{\eta}=e_1$, then $\eta = \eta_s^*$. Similarly, if $\eta = \eta_i^*$ then $\tilde{\eta} = e_1$. This implies that $\eta=\eta^*$ if and only if $\tilde{\eta}_s=e_1$. Thus, global stabilization of η_s^* in the η coordinates is equivalent to globally stabilization of the point e_1 in the $\tilde{\eta}_s$ coordinates.

Step 2. Error Dynamics: The dynamics of $\tilde{\eta}_s$ are given by

$$\dot{\tilde{\eta}}_s = \dot{\eta} \ominus \eta_s^{*c} + \eta \ominus \dot{\eta}_s^{*c} = \tilde{\eta}_s \ominus \eta_s^* \ominus (\alpha(w) - \eta_s^{*c} \ominus \dot{\eta}_s^*) \ominus \eta_s^{*c},$$

where $\alpha(w) := [0, w]^{\top}$. We can now select the feedback law $\alpha(w) := \eta_s^{*c} \ominus \dot{\eta}_s^* + \alpha(w_r)$ to obtain the error dynamics

$$\dot{\tilde{\eta}}_s = \tilde{\eta}_s \ominus \alpha(w_r) = -\omega_r R \tilde{\eta}_s, \quad \tilde{\eta}_s \in \mathbb{S}^1, \quad s \in \Omega,$$
 (54)

where we used the facts that $\eta_s^* \in \mathbb{S}^1$, and $\eta_s^{*c} \in \mathbb{S}^1$. Thus, robust global tracking of the signals η_s^* is equivalent to the robust global stabilization of the point e_1 in \mathbb{S}^1 for the error

Step 3. Robust Global Stabilization in \mathbb{S}^1 : To globally stabilize $e_1 \in \mathbb{S}^1$, each hybrid controller \mathcal{H}_s is endowed with a logic state $m \in M := \{0,1\}$ and feedback law $w_r = e_{m+1}^{\top} \tilde{\eta}_s$. Consider the sets

$$\tilde{C}_1 := \{ \tilde{\eta}_s \in \mathbb{S}^1 : \tilde{\eta}_s \le -1/3 \}, \ \tilde{C}_0 := \{ \tilde{\eta}_s \in \mathbb{S}^1 : \tilde{\eta}_s \ge -2/3 \},$$

and define $\tilde{D}_1:=\overline{\mathbb{S}^1\backslash \tilde{C}_1}$ and $\tilde{D}_0:=\overline{\mathbb{S}^1\backslash \tilde{C}_0}$. The flow set of the closed-loop system is given by

$$C_c := \left(\tilde{C}_1 \times \{1\}\right) \cup \left(\tilde{C}_0 \times \{0\}\right) \subset \mathbb{S}^1 \times M.$$

The jump set is given by

$$D_c := \left(\tilde{D}_1 \times \{1\} \right) \cup \left(\tilde{D}_0 \times \{0\} \right) \subset \mathbb{S}^1 \times M.$$

The jump map is given by $\tilde{\eta}_s^+ = \tilde{\eta}_s$ and $m^+ = 1 - m$, which toggles the value of m between 0 and 1. The flow map is given by $\hat{\eta}_s = -e_{m+1}^{\top} \hat{\eta}_s R \hat{\eta}_s$ and $\dot{m} = 0$. Note that when m = 1 the dynamics of $\tilde{\eta}_s$ satisfy $\dot{\tilde{\eta}}_{s,1} = \tilde{\eta}_{s,1} \tilde{\eta}_{s,2}$ and $\dot{\tilde{\eta}}_{s,2} = \tilde{\eta}_{s,1}^2$. Using the energy function $V_1 = 1 + \tilde{\eta}_{s,2}$, we have that $\dot{V}_1 = -(1 - 1)$ $\tilde{\eta}_{s,2}^2 \le 0$, which shows that the state $\tilde{\eta}_s$ converges to the point Re_1 provided $\tilde{\eta}_{s,1}(0) \neq 0$. Similarly, when m=0 we have that $\dot{\tilde{\eta}}_{s,1} = \tilde{\eta}_{s,2}^2$ and $\dot{\tilde{\eta}}_{s,2} = -\tilde{\eta}_{s,1}\tilde{\eta}_{s,2}$. Using $V_0 = 1 - \tilde{\eta}_{s,1}$

we get $\dot{V}_0 = -(1 - \tilde{\eta}_{s,1}^2) \le 0$ which shows that the state $\tilde{\eta}_s$ converges to the point e_1 provided $\tilde{\eta}_{s,2}(0) \neq 0$. Thus, by the construction of the flow and jump sets, the hybrid closedloop system guarantees global convergence of $\tilde{\eta}_s$ to the point $e_1 \in \mathbb{S}^1$, and indeed, UGAS of $\{e_1\} \times M$.

Having defined a controller for the linear velocity (53), and hybrid controllers \mathcal{H}_s for global reference tracking of the signals η_1^* and η_2^* , we proceed to construct a Hybrid Supervisor Control System that coordinates the switching of the state $s \in \Omega$ in order to achieve UGAS of a point $\gamma^* = [p^*, \eta^*]^\top$. Let $\varepsilon_2 > \varepsilon_1 > 0$. For s = 1 and $p^* \in \mathbb{R}^2$, consider the flow and jump sets

$$C_1(p^*) := \left(\mathbb{R}^2 \times C_c\right) \cap \left(\overline{(\mathbb{R}^2 \backslash p^* + \varepsilon_1 \mathbb{B})} \times \mathbb{S}^1 \times M\right),$$

$$D_1(p^*) := \left(\mathbb{R}^2 \times D_c\right) \cap \left(\overline{(\mathbb{R}^2 \backslash p^* + \varepsilon_1 \mathbb{B})} \times \mathbb{S}^1 \times M\right),$$

which allow flows and jumps outside of an ε_1 -neighborhood of the point p^* , and which drives the state η to η_1^* . For s=2, consider the flow and jump sets

$$C_2(p^*) := \left(\mathbb{R}^2 \times C_c\right) \cap \left((p^* + \varepsilon_2 \mathbb{B}) \times \mathbb{S}^1 \times M \right),$$

$$D_2(p^*) := \left(\mathbb{R}^2 \times D_c\right) \cap \left((p^* + \varepsilon_2 \mathbb{B}) \times \mathbb{S}^1 \times M \right),$$

which allow flows and jumps inside of an ε_2 -neighborhood of the point p^* , and which drives the state η to η_2^* . With these constructions at hand, we can now define the sets

$$H_1(p^*) := (p^* + \varepsilon_1 \mathbb{B}) \times \mathbb{S}^1 \times M,$$

$$H_2(p^*) := \overline{(\mathbb{R}^2 \backslash p^* + \varepsilon_2 \mathbb{B})} \times \mathbb{S}^1 \times M.$$

The toggle rule for the state $s \in \Omega$ is given by $J_s = 3 - s$. This construction guarantees that the controller s = 1 steers the position of the vehicle towards a ε_1 -neighborhood of u, and the angle of the vehicle towards $\eta_1^* = (z-p^*)/(z-p^*)$. Whenever z approaches p^* the controller switches to s=2 which steers the angle towards η_2^* . By the results of [46, Ex. 35], the second controller drives the orientation to a cone around η^* whose aperture converges to zero.

Finally, the closed-loop system can be written as (50) using $u = p^*, h = [m, s]^{\top}, \Theta = \mathbb{S}^1, \mathcal{T} := \{0, 1\} \times \{1, 2\}, \text{ the }$ mappings $F_h := \mathbf{0}_2$ and

$$f_{\gamma}:=\left[\begin{array}{c}\eta v\\-r(\gamma,h)R\eta_{s}\end{array}\right],\ r:=\ell(e_{m+1}^{\top}(\eta\ominus\eta_{s}^{*c}))\quad \text{(55a)}$$

$$G_h := \left[\begin{array}{c} 1 - m \\ s \end{array} \right] \bigcup \left[\begin{array}{c} m \\ 3 - s \end{array} \right], \tag{55b}$$

and the sets

$$\Psi_C^h(u) := \bigcup_{s \in \Omega} \left(C_s(u) \times \{s\} \right), \tag{56a}$$

$$\Psi_C^h(u) := \bigcup_{s \in \Omega} \left(C_s(u) \times \{s\} \right), \tag{56a}$$

$$\Psi_D^h(u) := \bigcup_{s \in \Omega} \left(\left(D_s(u) \cup H_s \right) \times \{s\} \right). \tag{56b}$$

Since the Hybrid Supervisor Control System satisfies all the Basic Assumptions (C1), (C2) and (C3), the resulting closedloop system is well-posed. Moreover, since the trajectories of the vehicle eventually enter and stay in the ball $u + \varepsilon_1 \mathbb{B}$ and the orientation η converges to a small neighborhood of η^* , the number of jumps is finite. Finally, by [46, Corollary 33], the compact set $\{\gamma^*\} \times \{0,1\} \times \{1,2\}$ is UGAS. We summarize with the following Proposition.

Proposition 2: For the constrained dynamics (52) the closed-loop system (55)-(56) satisfies Assumption 7. \diamondsuit

C. Multi-Time Scale Hybrid Source Seeking

Having designed a hybrid controller that guarantees robust global stabilization of a set point $p^*=u$ for the vehicle dynamics (49), we proceed to study the controller that regulates the set point u towards the maximizer of the potential field while avoiding the obstacle. We consider the hybrid source seeking dynamics of Section IV with state $z=[u^\top,q,\mu^\top]^\top\in\mathbb{R}^5$ and parameter $\varepsilon>0$, given by

$$\dot{z} = \varepsilon F_z(z, p) := \begin{bmatrix} -\varepsilon \mathcal{F}_q(p)\mu \\ 0 \\ \varepsilon \omega R\mu \end{bmatrix}, \ z \in C_z := C_{p,q} \times \mathbb{S}^1,$$
(57a)

$$z^{+} = G_{z}(z) := \left[u^{\top}, 3 - q, \mu^{\top} \right]^{\top}, \ z \in D_{z} := D_{p,q} \times \mathbb{S}^{1},$$
(57b)

where ε is a small tunable parameter that forces the flows of the hybrid controller to operate in a slower time scale compared to the dynamics (55). The following Theorem, which is the third main result of this paper, establishes obstacle avoidance and convergence of the mobile robot (49) towards a neighborhood of the source of the signal.

Theorem 3: Suppose that Assumption 1-4 and 7 hold, and consider the dynamics (49) interconnected with the hybrid controller \mathcal{H}_h . For each compact set $K_0 \subset \mathbb{R}^2 \backslash \mathbb{B}_{p_0,\rho}$ and $\nu > 0$ there exists $a^* > 0$ such that for each $a \in (0,a^*)$ there exists $\omega^* > 0$ such that for each $\omega > \omega^*$ there exists $\varrho^* > 0$ such that for each $\varrho \in (0,\varrho^*)$ there exists $\varepsilon^* > 0$ such that for each $\varepsilon \in (0,\varepsilon^*)$ each solution of the closed-loop system with $p(0,0) \in K_0$ and $|u(0,0)-p(0,0)| \leq \varrho$ generates trajectories p that: a) converge in finite time to the set $\mathcal{A}_J + (\nu + a)\mathbb{B}$; b) satisfy $p(t,j) \notin \mathcal{N}$ for all (t,j) in the domain of the solution.

Proof: Let $\kappa := [\gamma^\top, h^\top]^\top$. The closed-loop system in the $\varepsilon t = \tau$ time scale is given by the following hybrid system

$$\begin{array}{l} \dot{z} = F_z(z,\kappa) \\ \dot{\kappa} \in \frac{1}{\varepsilon} \left[\begin{array}{c} f_{\gamma}(\gamma,r(\kappa)) \\ \{\mathbf{0}_2\} \end{array} \right] \end{array} \right\}, \ (z,\kappa) \in C_z \times \Psi^h_C(u), \ \ (\mathbf{58a}) \\ z^+ = z \\ \kappa^+ \in \left[\begin{array}{c} \{\gamma\} \\ G_h(h) \end{array} \right] \end{array} \right\}, \ (z,\kappa) \in C_z \times \Psi^h_D(u), \ \ (\mathbf{58b}) \\ z^+ = G_z(z,\kappa) \\ \kappa^+ = \kappa \end{array} \right\}, \ (z,\kappa) \in D_z \times \Psi^h(u), \ \ (\mathbf{58c})$$

where $\Psi^h(u) := \Psi^h_D(u) \cup \Psi^h_D(u)$. System (58) is a singularly perturbed hybrid system with hybrid boundary layer dynamics and hybrid reduced dynamics [28]. To analyze this system, we first use $C'_z = (C_{u,q} + \delta \mathbb{B}) \times \mathbb{S}^1$ and $D'_z := (D_{u,q} + \delta \mathbb{B}) \times \mathbb{S}^1$ instead of C_z and D_z , with $\delta > 0$ sufficiently small. For this hybrid system the *hybrid boundary layer dynamics* [28, Sec.

III] in the t-time scale are given by $\dot{z}=\mathbf{0}_5$ and

$$\dot{\kappa} \in \begin{bmatrix} f_{\gamma}(\gamma, r(\kappa)) \\ \{\mathbf{0}_{2}\} \end{bmatrix} \right\}, (z, \kappa) \in C'_{z} \times \Psi_{C}^{h}(u), \quad (59a)$$

$$z^{+} = z$$

$$\kappa^{+} \in \begin{bmatrix} \{\gamma\} \\ G_{h}(h) \end{bmatrix} \right\}, (z, \kappa) \in C'_{z} \times \Psi_{D}^{h}(u), \quad (59b)$$

which, by Assumption 7, generates a well-defined slow average system, corresponding to the dynamics (57) with p replaced by u, and δ -inflated sets $C_{u,q}$ and $D_{u,q}$, which are precisely the hybrid dynamics (28) (with e=0) whose stabilizing properties were already established in Section IV. By the proof of Theorem 1, the slow-average system renders the set $\mathcal{A}:=\mathcal{A}_J\times\{1,2\}\times\mathbb{S}^1$ SGPAS as $(a,\omega)\to 0^+$. Then, by [28, Thm. 2] there exist $\tilde{\beta}\in\mathcal{KL}$ such that for each compact set $K\subset\mathcal{O}$ there exists $\varepsilon^*>0$ such that for each $\varepsilon\in(0,\varepsilon^*\}$ the following bound holds:

$$|\hat{z}(\varrho,k)|_{\mathcal{A}} \le \tilde{\beta}(|\hat{z}(0,0)|_{\mathcal{A}}, \varrho+k) + \frac{\nu}{4},\tag{60}$$

for all $(\varrho,k) \in \operatorname{dom}(\hat{z})$ with $u(0,0) \in K$, where \hat{z} is a mapping satisfying $\operatorname{graph}(\hat{z}) = \bigcup_{(t,j)\in\operatorname{dom}z}\{\varrho(t,j),k(t,j),z(t,j)\}$ where z is the component solution of system (58) with sets C'_z and D'_z , and where ϱ increases according to $\dot{\varrho}=1$ with the flows of the system, and k increases according to $k^+=k+1$ only with the jumps of (58c). Since the values of \hat{z} and z match by construction, and since the HDS does not generate purely discrete solutions, the bound (60) and the structure of the set $\mathcal A$ implies the existence of a T>0 such that

$$u(t,j) \in \mathcal{A}_J + \frac{\nu}{2} \mathbb{B},$$
 (61)

for all (t,j) in the domain of the solution satisfying $t+j \geq T$. Indeed, since each initial condition satisfying $u(0,0) \in K_0$ is complete, every solution from $K_0 \times \mathbb{S}^1 \times \Psi^h(u)$ converges to $\mathcal{A}_J + \frac{\nu}{2} \mathbb{B}$.

To establish obstacle avoidance and source seeking for the position p of the vehicle, we use closeness of the trajectories u and p whenever they are initialized sufficiently close to each other. By [29, Cor. 7.7], the infinite horizon reachable set from initial conditions $p(0,0),u(0,0)\in K_0$ is bounded and contained in some set $K_1\mathbb{B}$, with $K_1 > 0$. Let ν' satisfy $\nu' \in (0, \nu/2)$. By Assumption 7, when $\varepsilon = 0$ we have that $\dot{z}=0$ (and therefore $\dot{u}=0$) and there exists $\beta\in\mathcal{KL}$ such that the bound $|p(t,j) - u(t,j)| \le \beta(|p(0,0) - u(0,0)|, t+j)$ holds during the flows (58a) and jumps (58b) with u restricted to the compact set K_1 . Since the state κ evolves on a compact set there exists $\ell > 0$ such that $|F_z(z, \kappa)| \leq \ell$ for all $z \in K_0$. Thus, there exists $\varepsilon^{**} \in (0, \varepsilon^*)$ such that for all $\varepsilon \in (0, \varepsilon^{**})$ the flow map (57a) satisfies $\dot{z} \in \varepsilon \mathbb{B}$ and the following bound holds during flows (58a) and jumps (58b): $|p(t,j)-u(t,j)| \le \beta(|p(0,0)-u(0,0)|,t+j) + \nu'/2$. Since $\beta \in \mathcal{KL}$, there exists a $\varrho > 0$ sufficiently small such that $\beta(\varrho,0) \leq \nu'/2$. Therefore, if $|p(0,0)-u(0,0)| \leq \varrho$, we obtain that

$$|p(t,j) - u(t,j)| \le \nu' < \frac{\nu}{2},$$
 (62)

for all (t, j) along flows (58a) and jumps (58b). Since the jumps (58c) do not change the values of (u, p), the bound

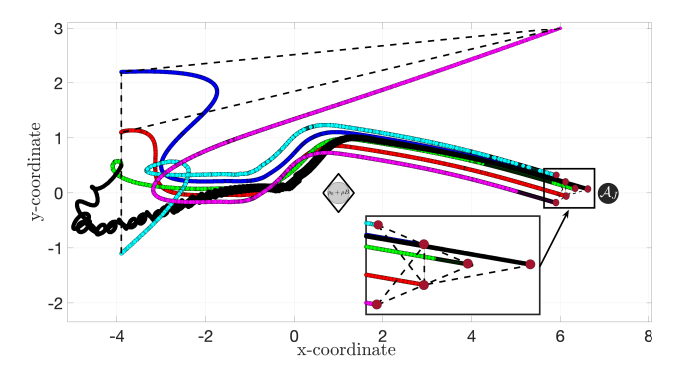


Fig. 6: Trajectories of the vehicles using a hybrid feedback navigation law. Each logic state eventually converges to 2.

(62) holds for the singularly perturbed hybrid system (58). Combining (62) and (61) we obtain convergence of p to a ν -neighbrhood of \mathcal{A}_J . Since u remains in $\operatorname{int}(\overline{\mathcal{O}})$, obstacle avoidance follows by ν -closeness between p and u.

To the knowledge of the authors, Theorem 3 is the first result in the literature of averaging-based source seeking that implements hybrid controllers in both the reduced dynamics of the system and the boundary layer dynamics. This methodology can also be applied to other mechanical and electrical systems that are not stabilizable by smooth feedback, including more complicated non-holonomic systems; see [47]. As in Theorems 1 and 2, well-posedness of the hybrid controller guarantees suitable robustness properties for the close-loop system. The multi-time scale approach can naturally be extended to MVS, where each vehicle is first stabilized using a hybrid controller whose reference is controlled using the cooperative hybrid controller studied in Section V. Finally, while the results of this paper have focused on the single obstacle case, extensions to the setting of multiple obstacles might be possible following the preliminary results of [48]. Future research will explore this approach.

VII. NUMERICAL AND EXPERIMENTAL RESULTS

In this section, we present some numerical and experimental results that illustrate the application of the hybrid adaptive controllers studied in the paper.

A. Source Seeking with Hybrid Leader and Followers

Consider a group of 6 vehicles with dynamics (2) aiming to achieve formation around the source of a signal J, which can be sensed only by the agent $S=\{4\}$, i.e., $\gamma=[0\ 0\ 0\ 1\ 0\ 0]$. For the purpose of simulation, we assume that the potential field has a quadratic form $J=\frac{1}{2}(x_1-7)^2+\frac{1}{2}y_1^2$, with maximum at the point $p^*=[7,0]^\top$. There is an obstacle located at the point $p_0=[1,0]^\top$, modeled by a circle with radius r=0.1. To test the performance of the algorithm, we initialize some of the followers at the left hand side of the obstacle and some at the right hand side. The communication links are characterized by an undirected graph $\mathcal G$ described by a ring, and the desired formation is characterized by the vectors $x_f:=0.25[0,0,\frac{\sqrt{3}}{2},2,\frac{-\sqrt{3}}{2},\frac{\sqrt{3}}{2}]^\top$ and $y_f:=0.25[0,-1,-0.5,-0.5,0.5,-1.5]^\top$. The parameters of the

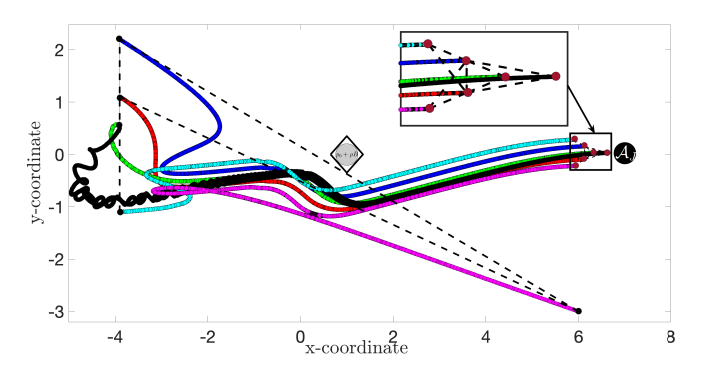


Fig. 7: Trajectories vehicles using a hybrid feedback navigation law. Each logic state eventually converges to 1.

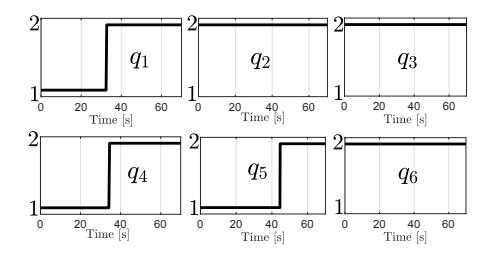


Fig. 8: Evolution in time of the logic states q_i associated to the trajectories of Fig. 6.

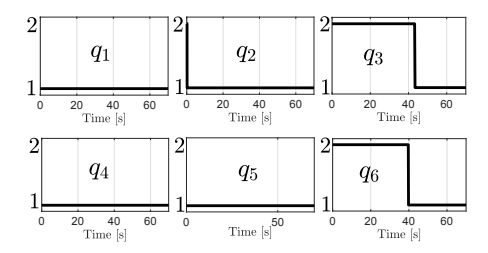


Fig. 9: Evolution in time of the logic states q_i associated to the trajectories of Fig. 7.

controllers are selected as $\rho_i = 0.4$, $\lambda_i = 0.09$, $\mu_i = 1.1$, $a_i = 0.01, \ \bar{\omega}_i = 1, \ k_i = 1, \ \omega_i = 150, \ \text{and} \ \sigma = 1.$ Figures 6 and 7 show two different trajectories of the multivehicle system generated from two different initial conditions, and corresponding to solutions of the hybrid source seeking controllers (34). The dotted lines show the communication graph between the agents, and the inset shows the desired formation achieved in a neighborhood of the position of the source A_J . Since $\gamma_4 = 1$, only agent 4 is sensing the potential J by means of the the first term in (34). However, all the vehicles implement hybrid dynamics to avoid the obstacle. Note that the two different initializations of Figures 6 and 7 generate switching behaviors fundamentally different. Namely, trajectories associated to Figure 6 generate states q_i that eventually switch to $q_i = 2$ for all $i \in \mathcal{V}$, while the trajectories associated to Figure 7 generate states q_i that eventually switch to $q_i = 1$ for all $i \in \mathcal{V}$. This behavior is shown in Figure 9.

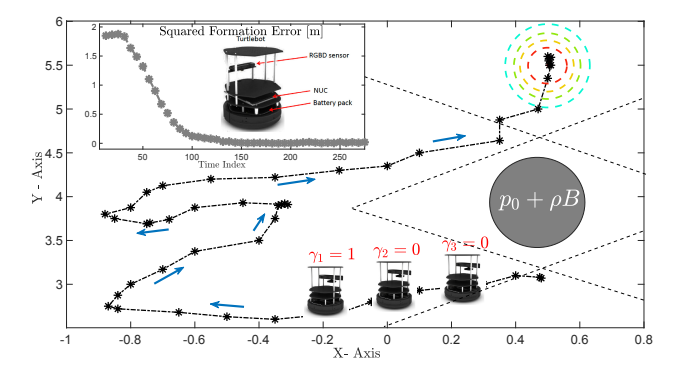


Fig. 10: Experimental results with Turtlebot platform. The trajectory of the leader (agent 1) is shown with dashed lines. The inset shows the squared formation error for the MVS.

B. Experimental Results

In order to test the practical viability of the theoretical results presented in this paper, the hybrid model-free controller was implemented on a fleet of three nonholonomic TurtleBots, one of which is shown in the inset of Figure 10. Each of the robots has an RGBD camera sensor to localize itself in the environment and to detect potential obstacles, a NUC computer running on Robot Operating System (ROS), and a Lithium-Ion battery of 14.8 V, which allows an average operating time of 5 hours. The robots run a dedicated particle filter algorithm on the RGBD sensor's data to localize itself in a pre-uploaded map of the environment where the position of the source of the signal is unknown. In this special case, the followers only focus on maintaining a formation defined as a line. The coefficients of the controllers implemented in the hardware are the same as in the previous Subsection, with the difference that the gains k_i of the followers are selected much larger than the gain of the leader. As in Figure 1, the positions of the three vehicles are initialized sufficiently close to each other. The source is located at the point $p^* = [0.5, 5.5]^{\top}$. The trajectory of the leader vehicle is illustrated in Figure 10, which also illustrates the virtual covering induced by the sets \mathcal{O}_1 and \mathcal{O}_2 of equation (14). The inset of Figure 10 also shows the squared formation error for the MVS. It can be observed that robots converge to the maximizer of the potential field following a trajectory that avoids the obstacle.

VIII. CONCLUSIONS AND OUTLOOK

We presented a novel model-free hybrid controller designed to coordinate a group of multiple autonomous vehicles towards the source of a signal whose position is unknown, but whose intensity can be sensed by a subset of the vehicles, while simultaneously avoiding an obstacle. The hybrid law induces a switching behavior in the control system of each of the vehicles, guaranteeing robust obstacle avoidance under a class of arbitrarily small adversarial jamming signals. By using tools from singularly perturbed hybrid dynamical systems, we showed that these dynamics can be applied to vehicles with general nonlinear dynamics that are stabilizable by hybrid feedback. Numerical and experimental results were also presented. Future directions will focus on multi-obstacle

avoidance problems with unknown obstacle locations, and hybrid adaptive controllers with temporal logic specifications.

ACKNOWLEDGMENTS

The authors would like to thank the Associate Editor and the anonymous reviewers for several constructive comments that were instrumental to improve the quality of the manuscript.

REFERENCES

- S. Azuma, M. S. Sakar, and G. J. Pappas, "Stochastic source seeking by mobile robots," *IEEE Transactions on Automatic Control*, vol. 57, no. 9, pp. 2308–2321, 2012.
- [2] E. Ramirez-Llanos and S. Martinez, "Stochastic source seeking for mobile robots in obstacle environments via the SPSA method," *IEEE Trans. on Automatic Control*, vol. 64, no. 4, pp. 1732–1739, 2018.
- [3] S. Z. Khong, Y. Tan, C. Manzie, and D. Nešíc, "Multi-agent source seeking via discrete-time extremum seeking control," *Automatica*, pp. 2312– 2320, 2014
- [4] E. Biyik and M. Arcak, "Gradient climbing in formation via extremum seeking and passivity-based coordination rules," *Asian Journal of Control*, vol. 10, no. 2, pp. 201–211, 2008.
- [5] K. Ariyur and M. Krstic, Real-Time Optimization by Extremum-Seeking Control. Hoboken, NJ: Wiley, 2003.
- [6] N. Ghods, Extremum Seeking for Mobile Robots. University of California at Santa Diego, 2011.
- [7] C. Zhang, D. Arnold, N. Ghods, A. Siranosian, and M. Krstić, "Source seeking with non-holonomic unicycle without position measurement and with tuning of forward velocity," *Systems and Control Letters*, vol. 56, no. 3, pp. 245–252, 2007.
- [8] Y. Zhang, O. Makarenkov, and N. Gans, "Extremum seeking control of a nonholonomic system with sensor constraints," *Automatica*, vol. 70, pp. 86–93, 2016.
- [9] H. Dürr, M. S. Stanković, D. V. Dimarogonas, C. Ebenbauer, and K. H. Johansson, "Obstacle avoidance for an extremum seeking system using a navigation function," *In proc. of American Control Conference*, pp. 4062–4067, 2013.
- [10] C. Zhang, A. Siranosian, and M. Krstić, "Extremum seeking for moderately unstable systems and for autonomous vehicle target tracking without position measurements," *Automatica*, pp. 1832–1839, 2007.
- [11] A. S. Matveev, M. C. Hoy, and A. V. Savkin, "3D environmental extremum seeking navigation of a nonholonomic mobile robot," *Automatica*, vol. 50, pp. 1802–1815, 2014.
- [12] H. Dürr, M. Krstic, A. Scheinker, and C. Ebenbauer, "Extremum seeking for dynamic maps using liebrackets and singular perturbations," *Automatica*, vol. 83, no. 91-99, 2017.
- [13] C. Li, Z. Qu, and M. A. Weitnauer, "Distributed extremum seeking and formation control for nonholonomic mobile network," *Systems & Control Letters*, vol. 75, pp. 27–34, 2015.
- [14] R. Suttner and Z. Sun, "Exponential and practical exponential stability of second-order formation control system," *IEEE Conf. on Decision and Control*, pp. 3521–3526., 2019.
- [15] Z. Li, H. You, and S. Song, "Cooperative source seeking via networked multi-vehicle systems," *Automatica*, vol. 115, 2020.
- [16] J. I. Poveda, M. Benosman, and A. R. Teel, "Distributed extremum seeking in multi-agent systems with arbitrary switching graphs," 20th IFAC World Congress, vol. 50, no. 1, pp. 735–740, 2017.
- [17] D. E. Koditschek and E. Rimon, "Robot navigation functions on manifolds with boundary," *Advances in Applied Mathematics*, vol. 11, pp. 412–442, 1990.
- [18] R. Sanfelice, Robust Hybrid Control Systems. University of California at Santa Barbara. 2007.
- [19] E. D. Sontag, "Stability and stabilization: discontinuities and the effect of disturbances," *Nonlinear Analysis, Differential Equations and Control*, pp. 551–598, 1989.
- [20] A. R. Teel, L. Moreau, and D. Nesic, "A unified framework for input-to-state stability in systems with two time scales," *IEEE Transactions on Automatic Control*, pp. 1526–1544, 2003.
- [21] S. Paternain, D. Koditschek, and A. Ribeiro, "Navigation functions for convex potentials in a space with convex obstacles," *IEEE Transactions* on Automatic Control, vol. 63, no. 4, pp. 2944–2959, 2018.
- on Automatic Control, vol. 63, no. 4, pp. 2944–2959, 2018.
 [22] A. Zuyev and V. Grushkovskaya, "Obstacle avoidance problem for driftless nonlinear systems with oscillating controls," 20th IFAC World Congress, vol. 50, no. 1, pp. 10476–10481, 2017.

- [23] C. Belta, V. Isler, and G. Pappas, "Discrete abstractions for robot motion planning and control in polygonal environments," *IEEE Trans.* on Automatic Control, vol. 21, no. 5, pp. 864–874, 2005.
- [24] A. D. Ames, J. W. Grizzle, and P. Tabuada, "Control barrier function based quadratic programs for safety critical systems," *IEEE Transactions* on Automatic Control, vol. 62, no. 8, pp. 3861–3876, 2017.
- [25] S. Paternain and A. Ribeiro, "Stochastic artificial potentials for online safe navigation," *IEEE Trans. Autom. Contr.*, vol. 65, no. 5, pp. 1985– 2000, 2020.
- [26] J. I. Poveda, M. Benosman, A. R. Teel, and R. G. Sanfelice, "A hybrid adaptive feedback law for robust obstacle avoidance and coordination in multiple vehicle systems," in Proc. of American Control Conference, pp. 616–621, 2018.
- [27] J. P. Hespanha and A. Morse, "Stabilization of nonholonomic integrators via logic-based switching," *Automatica*, vol. 35, no. 3, pp. 385–393, 1999.
- [28] W. Wang, A. R. Teel, and D. Nešíc, "Averaging in singularly perturbed hybrid systems with hybrid boundary layer systems," 51st IEEE Conference on Decision and Control, pp. 6855–6860, 2012.
- [29] R. Goebel, R. Sanfelice, and A. R. Teel, Hybrid Dynamical System. Princeton, NJ: Princeton University Press, 2012.
- [30] B. D. Craven and B. M. Glover, "Invex functions and duality," J. Austral. Math. Soc. (Series A), vol. 39, pp. 1–20, 1985.
- [31] J. Cochran and M. Krstić, "Nonholonomic source seeking with tuning of angular velocity," *IEEE Trans. on Automatic Control*, vol. 54, no. 4, pp. 717–731, 2009.
- [32] D. Nešić, Y. Tan, W. Moase, and C. Manzie, "A unifying approach to extremum seeking: Adaptive schemes based on estimation of derivatives," in Proc. of IEEE Conference on Decision and Control, 2010.
- [33] A. F. Filippov, Differential Equations with Discontinuous Right-hand Sides. Kluwer, 1988.
- [34] R. G. Sanfelice, M. J. Messina, S. E. Tuna, and A. R. Teel, "Robust hybrid controllers for contrinuous-time systems with applications to obstacle avoidance and regulation to disconnected set of points," *In Proc.* of American Control Conference, pp. 3352–3357, 2006.
- [35] C. G. Mayhew and A. R. Teel, "Synergistic hybrid feedback for global rigid-body attitude tracking on so(3)," *IEEE Transactions on Automatic* Control, vol. 58, no. 11, pp. 2730–2742, 2013.
- [36] M. Maghenem and R. G. Sanfelice, "Barrier function certificates for forward invariance in hybrid inclusions," *IEEE Conf. on Decision and Control*, pp. 759–764, 2018.
- [37] J. I. Poveda and A. R. Teel, "A framework for a class of hybrid extremum seeking controllers with dynamic inclusions," *Automatica*, vol. 76, pp. 113–126, 2017.
- [38] J. I. Poveda, R. Kutadinata, C. Manzie, D. Nešić, A. R. Teel, and C. K. Liao, "Hybrid extremum seeking for black-box optimization in hybrid plants: An analytical framework," *IEEE Conference on Decision and Control*, pp. 2235–2240, 2018.
- [39] W. Wang, A. R. Teel, and D. Nešić, "Analysis for a class of singularly perturbed hybrid systems via averaging," *Automatica*, pp. 1057–1068, 2012
- [40] J. I. Poveda and N. Li, "Robust hybrid zero-order optimization algorithms with acceleration via averaging in time," *Automatica*, vol. 123, 2021.
- [41] J. I. Poveda and A. R. Teel, "Hybrid mechanisms for robust synchronization and coordination of multi-agent networked sampled-data systems," *Automatica*, vol. 99, pp. 41–53, 2019.
- [42] M. Mesbahi and M. Egerstedt, Graph Theoretic Methods in Multiagent Networks. Princeton Series, 2010.
- [43] A. R. Teel, R. G. Sanfelice, and R. Goebel, Hybrid Control Systems, pp. 4671–4696. New York, NY: Encyclopedia of Complexity and Systems Science. 2009.
- [44] S. Zhao, D. V. Dimarogonas, Z. Sun, and D. Bauso, "A general approach to coordination control of mobile agents with motion constraints," *IEEE Transactions on Automatic Control*, vol. 63, no. 5, pp. 1509–1516, 2018.
- [45] R. W. Brockett, "Asymptotic stability and feedback stabilization," Differential Geometric Control Theory, vol. 27, no. 1, pp. 181–191, 1983.
- [46] R. Goebel, R. G. Sanfelice, and A. R. Teel, "Hybrid dynamical systems," IEEE Control Systems Magazine, vol. 29, no. 2, pp. 28–93, 2009.
- [47] R. M. Murray, Z. Li, and S. S. Sastry, A Mathematical Introduction to Robotic Manipulation. CRC Press, 1994.
- [48] V. Muthukumaran, R. G. Sanfelice, and G. H. Elkaim, "A hybrid control strategy for autonomous navigation while avoiding multiple obstacles at unknown locations," *IEEE 15th International Conference on Automation Science and Engineering*, pp. 1042–1047, 2019.



Jorge I. Poveda is an Assistant Professor in the Department of Electrical, Computer, and Energy Engineering at the University of Colorado, Boulder. He received the M.Sc. and Ph.D. degrees in Electrical and Computer Engineering from the University of California at Santa Barbara in 2016 and 2018, respectively. He was a Postdoctoral Fellow at Harvard University in 2018, and a research intern at the Mitsubishi Electric Research Laboratories (MERL) during the summers of 2016 and 2017. He holds double

degrees in Mechanical Engineering and Electronics Engineering from the University of Los Andes, Colombia. He has received the CCDC Outstanding Scholar Fellowship at UC Santa Barbara, and he was a Best Student Paper Award Finalist in the 2017 IEEE Conference on Decision and Control. In 2020, he received the Research Initiation Initiative Award (CRII) by the National Science Foundation (NSF).



Mouhacine Benosman is a Senior Research Scientist at Mitsubishi Electric Research Labs (MERL) in Cambdrige, USA. He has received his Ph.D. in 2002 from Ecole Centrale de Nantes, France. Before joining MERL he worked at Reims University, France, Strathclyde University, Scotland, and National University of Singapore. His research interests include multi-agent distributed control with applications to robotics and smart-grids, control of infinite dimensional systems with applications to fluid dynamics, and

learning and adaptive control. He is an Associate Editor for IEEE Control Systems Letters, and for the Journal of Opt. Theory and Applications. He is a Senior Editor of the Inter. Journal of Adaptive Control and Signal Processing.



Andrew R. Teel received his A.B. degree in Engineering Sciences from Dartmouth College, New Hampshire, in 1987, and his M.S. and Ph.D. degrees in Electrical Engineering from the University of California, Berkeley, in 1989 and 1992, respectively. After receiving his Ph.D., he was a postdoctoral fellow at the Ecole des Mines de Paris in Fontainebleau, France. He is currently a Distinguished Professor and Director of the Center for Control, Dynamical systems, and Computation at the University of California,

Santa Barbara. His research interests are in nonlinear and hybrid dynamical systems. He has received the NSF Research Initiation Award, the CAREER Award, the 1998 IEEE Leon K. Kirchmayer Prize Paper Award, the 1998 George S. Axelby Outstanding Paper Award, the first SIAM Control and Systems Theory Prize in 1998, the 1999 Donald P. Eckman Award, and the 2001 O. Hugo Schuck Best Paper Award. He also received in 2010 the IEEE Control Systems Magazine Outstanding Paper Award. He is the Editor-in-Chief of Automatica, and a Fellow of the IEEE and of IFAC.



Ricardo G. Sanfelice received the M.S. and Ph.D. degrees in electrical and computer engineering from the University of California, Santa Barbara, in 2004 and 2007, respectively. In 2007 and 2008, he held postdoctoral positions at the Laboratory for Information and Decision Systems, Massachusetts Institute of Technology, Cambridge, and at the Centre Automatique et Systèmes, École de Mines de Paris, Paris, France. Since 2014 he is with the Computer Engineering Department, University of California,

Santa Cruz, where he is a Professor and Director of the Cyber-Physical Systems Research Center. His research interests are in modeling, stability, robust control, observer design, and simulation of nonlinear and hybrid systems with applications to power systems, aerospace, and biology. Dr. Sanfelice is the recipient of the 2013 SIAM Control and Systems Theory Prize, the National Science Foundation CAREER award, the Air Force Young Investigator Research Award, and the 2010 IEEE Control Systems Magazine Outstanding Paper Award.